Evaluating effective stress parameters and undrained shear strength of soft-firm clays from CPT and DMT

Mayne, P.W. (2016). Invited keynote: Evaluating effective stress parameters and undrained shear strength of soft-firm clays from CPT and DMT. *In Pursuit of Best Practices - Proc. 5th Intl. Conf. on Geotechnical & Geophysical Site Characterization* (ISC-5, Jupiters Resort, Gold Coast, Australian Geomechanics Society, Vol. 1: 19-40

Mayne, P.W. (2016). Evaluating effective stress parameters and undrained shear strength of soft-firm clays from CPT and DMT. *Australian Geomechanics Journal* 51 (4): 27-55.

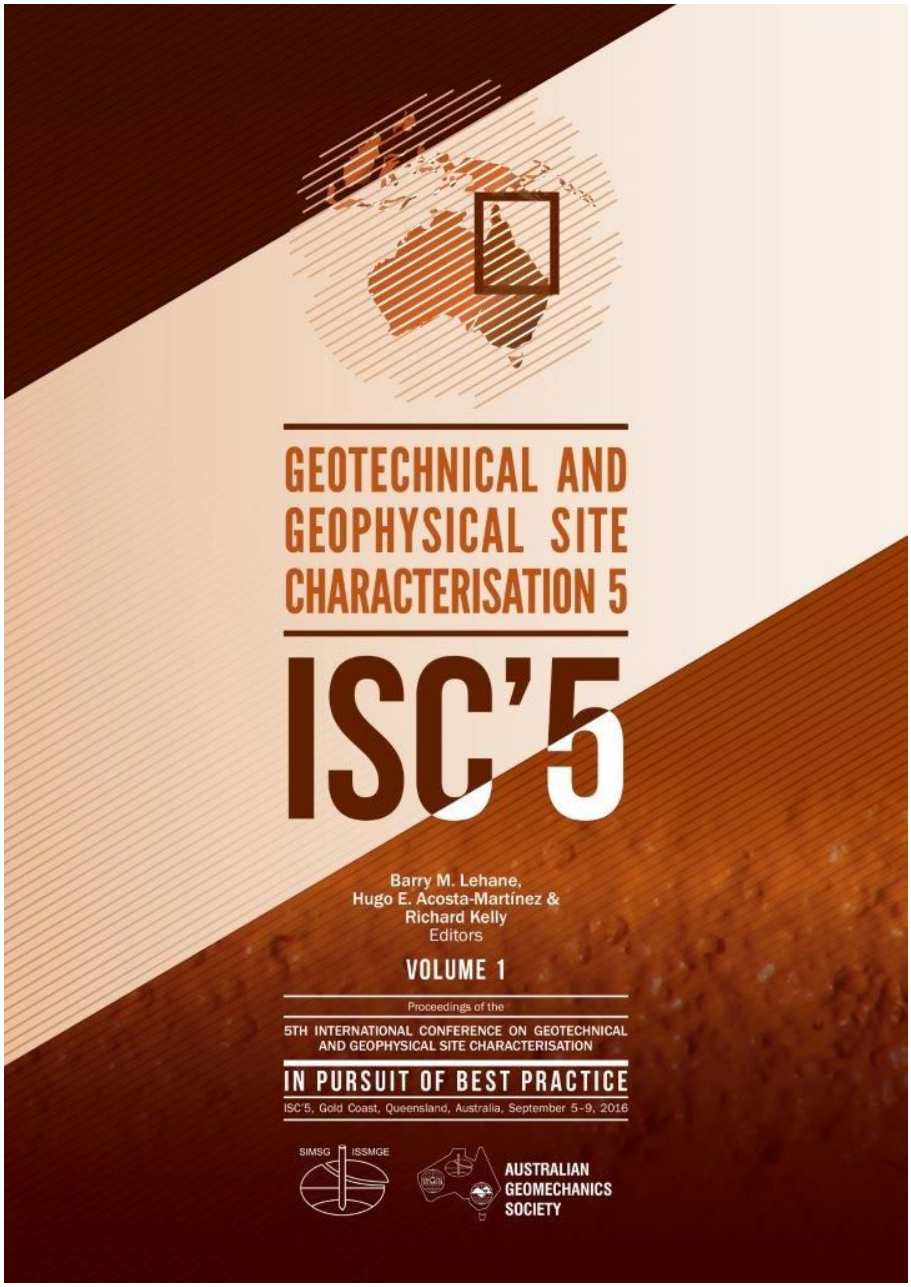

Evaluating effective stress parameters and undrained shear strengths of soft-firm clays from CPTu and DMT

P.W. Mayne
Georgia Institute of Technology, Atlanta, Georgia, USA

ABSTRACT: Results from piezocone penetration (CPTu) and flat dilatometer tests (DMT) can be used to evaluate the stratigraphy, soil types, and a suite of engineering parameters that are needed for geotechnical analysis and design, especially for finite element methods (FEM). Of particular interest herein is the utilization of in-situ test data for assessing the effective stress strength envelope (c' and ϕ') in soft to firm clays, as well as undrained shear strengths (s_u), since many FEM codes have built-in constitutive soil models that are based on critical-state soil mechanics and require effective stress parameters as input. An existing undrained limit plasticity solution for evaluating ϕ' in clays from CPTu is reviewed and then extended to the DMT via a link established thru spherical cavity expansion theory. Laboratory and field results on soft Bothkennar clay at the British national test site and additional CPTu data in clays are used to illustrate the methodologies.

1 INTRODUCTION

1.1 *Site investigation*

Soft to firm clays are commonly found offshore and onshore in marginal areas of construction, particularly coastal regions, lakeshores, and near waterways and rivers. As a result, construction concerns arise concerning suitable bearing capacity of shallow and deep foundations, stability of embankments, earth-retention walls, and excavations, as well as issues related to time rate of consolidation and long-term settlements. While laboratory testing programs are necessary, in-situ measurements from piezocone and dilatometer soundings allow the fast collection of data on these soft soils with immediate applications for the evaluation of geoengineering parameters for analysis and design.

1.2 *Geoparameters from CPT*

A fairly good number of soil engineering parameters have been defined and identified in order to represent the complexities of soil behavioral characteristics. A set of common-used and necessary geoparameters obtained from cone penetration testing (CPT) for analyses is listed in Table 1, yet this is far from a complete and comprehensive listing of all that have been implemented in practice (Lunne et al. 1997; Mayne 2007).

Readings from the CPT can include: cone resistance (q_t), sleeve friction (f_s), and penetration porewater pressure (u_2), as well as time to reach 50% consolidation during dissipation (t_{50}) and downhole shear wave velocity (V_s), thus designated SCPTù. The SCPTù is a particularly efficient and expedient means for site-specific subsurface investigations, as multiple measurements are collected from a single sounding as depicted in Figure 1. At a standard rate of push of 20 mm/s, the q_t, f_s, and u_2 readings are taken every 10 to 50 mm, while the t_{50} and/or V_s can be obtained every one meter.

Table 1. Common geoparameters for representing the behavior of soft-firm clays from CPT data

Symbol	Parameter	Readings
SBT	Soil behavior type	Uses CPT index I_c
I_c	CPT material index	I_c = *fctn* (Q_{tn} and F)
γ_t	Unit weight	from f_s reading
σ_{vo}	Overburden stress	$\sigma_{vo} = \int \gamma_t \, dz$
u_0	Hydrostatic pressure	Δu dissipations
σ_{vo}'	Effective stress	$\sigma_{vo}' = \sigma_{vo} - u_0$
σ_p'	Preconsolidation stress	$\sigma_p' = fctn\ (q_{net}, I_c)$
YSR	Yield stress ratio	YSR = σ_p'/σ_{vo}'
c'	Effective cohesion intercept	NTH method
ϕ'	Effective friction angle	NTH method
s_u	Undrained shear strength	N_{kt} factor
D'	Constrained modulus	D' $\approx 5 \cdot q_{net}$
G_0	Small-strain modulus	V_s data
G	Shear modulus	G_0 and τ/τ_{max}
c_{vh}	Coefficient of consolidation	Δu dissipation
K_0	Lateral stress coefficient	ϕ' and YSR
k	Hydraulic conductivity	Δu dissipations

Notes: NTH = Norwegian Institute of Technology; τ/τ_{max} = mobilized strength; τ = shear stress; τ_{max} = shear strength.

The penetrometer readings provide the net cone resistance ($q_{net} = q_t - \sigma_{vo}$) and excess porewater pressure ($\Delta u = u_2 - u_0$), as well as the effective cone tip resistance ($q_E = q_t - u_2$). Dimensionless CPT parameters have been developed to give: (a) normalized cone tip resistance: $Q = q_{net}/\sigma_{vo}'$, (b) normalized sleeve friction: $F = 100 \cdot f_s/q_{net}$, and (c) normalized porewater pressure parameter: $B_q = \Delta u/q_{net}$. Later, an updated version of Q is detailed and designated Q_{tn} that is needed in determining the CPT material index (I_c) which finds application in soil behavioral classification (Robertson 2009), as well as the assessment of the yield stress or preconsolidation stress (σ_p') and other geoparameters (Mayne 2015).

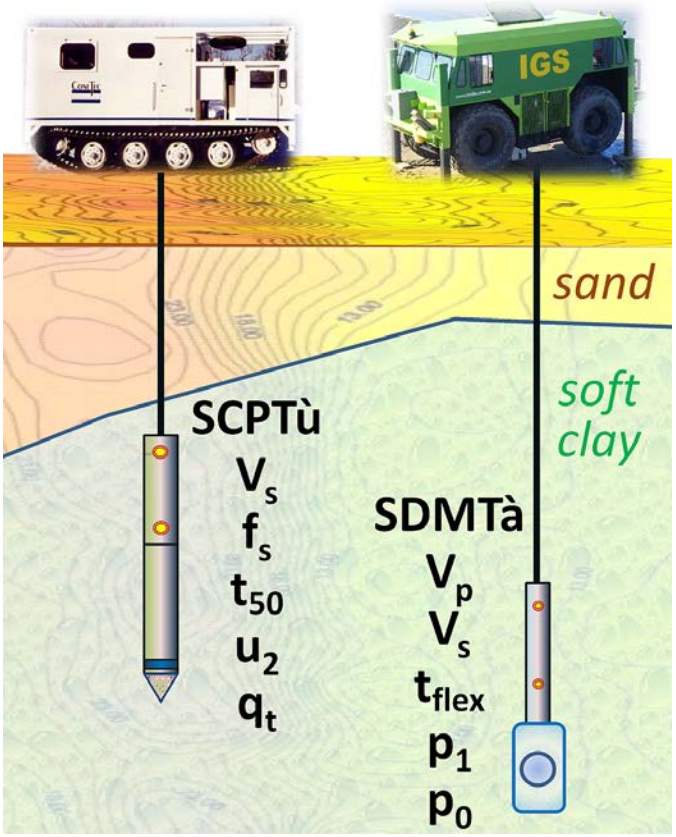

Figure 1. Multiple readings captured by a single sounding using seismic piezocone (SCPTù) and seismic dilatometer (SDMTà).

1.3 *Geoparameters from DMT*

A similar suite of geoparameters is found from the results of flat plate dilatometer tests (DMT), as initially identified by Marchetti (1980). In the DMT, two pressure readings are taken at each 0.2-m depth interval: (a) A-reading corrected to p_0 (contact pressure); and (b) B-reading corrected to p_1 (expansion pressure). These provide three DMT indices: (1) soil material index: $I_D = (p_1-p_0)/(p_0-u_0)$; (2) dilatometer modulus: $E_D = 34.7 \cdot (p_1-p_0)$; and (3) horizontal stress index: $K_D = (p_0-u_0)/\sigma_{vo}'$.

Additional readings can be taken during the DMT, including: (a) dissipation A-readings to get time for degree of consolidation (e.g., t_{flex}), (b) P-wave arrival to obtain V_p = compression wave velocity; (c) S-wave arrival to obtain V_s = shear wave velocity (Marchetti et al. 2008); (d) C-readings which are the membrane position of A-reading but taken during deflation, and (e) blade thrust readings. For the set of p_0, p_1, t_{flex}, V_p, and V_s measurements, the test can be designated SDMTà (Figure 1).

Details concerning the interpretation of soil engineering parameters from the DMT are provided in Marchetti et al. (2001) and Marchetti (2015). Two geoparameters which have not been evaluated in soft to firm clays using the DMT include: (1) effective stress friction angle (ϕ') and (2) effective cohesion intercept (c'). A methodology for their assessment from DMT readings in clay is proposed herein.

2 SOIL CLASSIFICATION BY CPT

2.1 *Soil behavioral type*

During CPT, soil types are usually identified indirectly since samples are not normally taken. The soil types can be assessed using one or more different approaches that rely on the direct measurements or post-processed readings, as indicated in Table 2. An alternative means to classify soil types in-situ is via the vision cone (VisCPT) whereby a video-cam records the images of soil particles passing a sapphire window (Ghalib et al. 2000).

Table 2. Methods for Soil Type Identification by CPT

Method	Procedure	Reference
"Rules of Thumb"	1. Clean sands: $q_t > 50\ \sigma_{atm}$ $u_2 \approx u_0$ 2. Clays: $q_t < 50\ \sigma_{atm}$ 2.1 Intact: $u_2 > u_0$ 2.2 Fissured: $u_2 < 0$	Mayne, et al. (2002)
Soil behavioral charts	Non-normalized: 1. q_t vs f_s 2. $(q_t - u_2)$ vs. f_s	Fellenius & Eslami (2000)
Soil behavioral charts	Normalized charts: 1. Q vs F 2. Q vs B_q	Lunne et al. (1997)
Soil behavior type (SBT)	CPT material index. I_c where $I_c = fctn(Q_{tn}, F)$	Robertson (2009)
Probability based relationships	Statistical estimates of sand, silt, and clay contents	Tümay, et al. (2011)

One of the most popular methods in use today utilizes soil behavioral type (SBT) charts based on Q, F, and B_q, termed *SBTn* since the three piezocone readings are normalized. This system classifies soils into 9 distinct zones that are presented in either log Q vs. log F charts or log Q vs B_q charts, or both (Lunne et al. 1997). The general layout for the Q-F chart is shown in Figure 2.

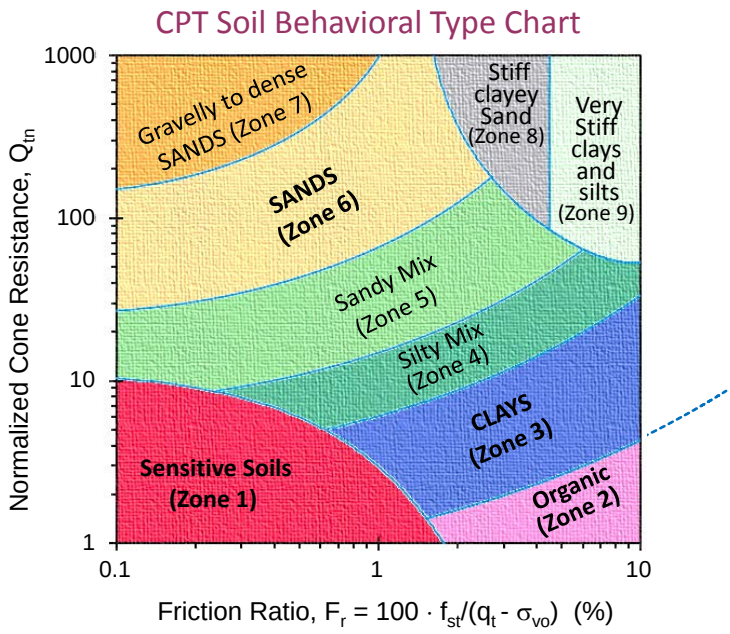

Figure 2. Chart for 9-zonal soil behavioral types from CPTu Q versus F (after Robertson 2009)

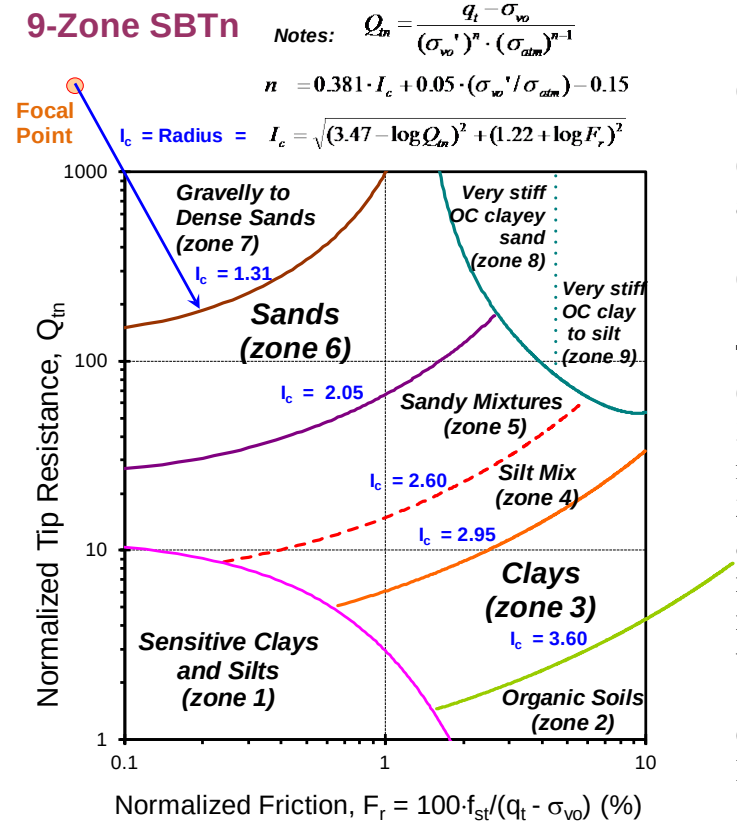

Figure 3. Definition of CPT material index I_c for Q versus F chart (after Robertson 2009)

2.2 *CPT material index, I_c*

The CPT material index I_c represents a family of the radii of a sets of circles which separate soil behavioral zones 2 through 7 in the log Q vs. log F chart, as shown by Figure 3. The index is given by:

$$I_c = \sqrt{(3.47 - \log Q)^2 + (1.22 + \log F)^2} \quad (1)$$

using the initial values of Q and F described previously. Then, a revised value of normalized cone resistance is defined:

$$Q_{tn} = \frac{(q_t - \sigma_{vo})/\sigma_{atm}}{(\sigma_{vo}'/\sigma_{atm})^n} \quad (2)$$

where the exponent "n" is determined from (Robertson 2009):

$$n = 0.381 \cdot I_c + 0.05 \cdot (\sigma_{vo}'/\sigma_{atm}) - 0.05 \leq 1.0 \quad (3)$$

and the index I_c is recalculated. Iteration converges quickly and generally only 3 cycles are needed to secure the operational I_c at each depth.

Algorithms are available to cull the CPTu data for zone 1 (soft sensitive clays) and zones 8 and 9 (stiff overconsolidated clays and sands). Once these three zones are identified, the material index I_c is used to separate zones 2 through 7, so all easily implemented on a spreadsheet or programmable software code.

Sensitive clays of Zone 1 are identified when:

$$Q_{tn} < 12 \cdot \exp(-1.4 \cdot F) \quad (4)$$

Overconsolidated soils of Zone 8 ($1.5 < F < 4.5\%$) and Zone 9 ($F \geq 4.5\%$) are found when:

$$Q_{tn} \geq [0.006(F-0.9) - 0.0004(F-0.9)^2 - 0.002]^{-1} \quad (5)$$

Then, the remaining soil types are identified by the CPT material index: Zone 2 (organic soils: $I_c \geq 3.60$); Zone 3 (clays: $2.95 \leq I_c < 3.60$); Zone 4 (silt mixtures: $2.60 \leq I_c < 2.95$); Zone 5 (sand mixtures: $2.05 \leq I_c < 2.60$); Zone 6 (sands: $1.31 \leq I_c < 2.05$); and Zone 7 (gravelly to dense sands: $I_c \leq 1.31$). The red dashed line at $I_c = 2.60$ represents an approximate boundary separating *drained* ($I_c < 2.60$) from undrained behavior ($I_c > 2.60$).

A similar CPTu material index has been developed for the 9 SBTn zones to represent the log Q vs. B_q diagrams, designated $I_{Q\text{-}Bq}$ by Torrez-Cruz (2015).

An alternate means to normalize the porewater pressures readings is through the parameter $\Delta u/\sigma_{vo}'$ that is used by Schneider et al. (2008) where the graph of log Q vs $\Delta u/\sigma_{vo}'$ provides various soil behavioral type zones. Schneider et al. (2012) derive corresponding equations that delineate the SBTs for both the Q-F and Q-$\Delta u/\sigma_{vo}'$ plots. They also provide data from a variety of field sites to populate the graphs and show the regions of drained, partially drained, and undrained behavior.

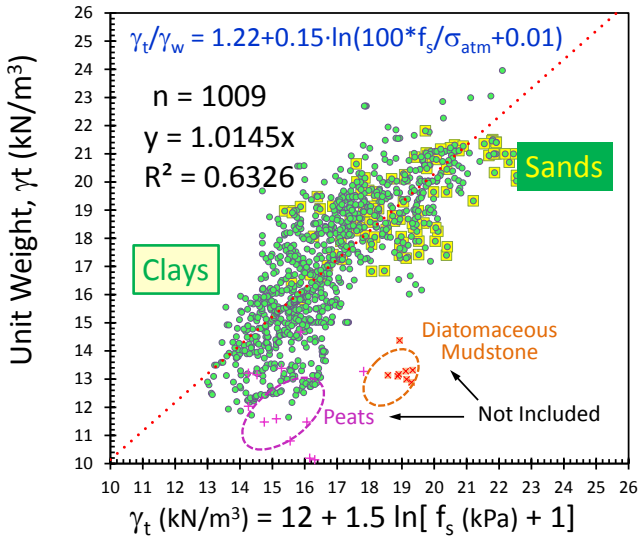

Figure 4. Soil unit weight from CPT sleeve friction reading

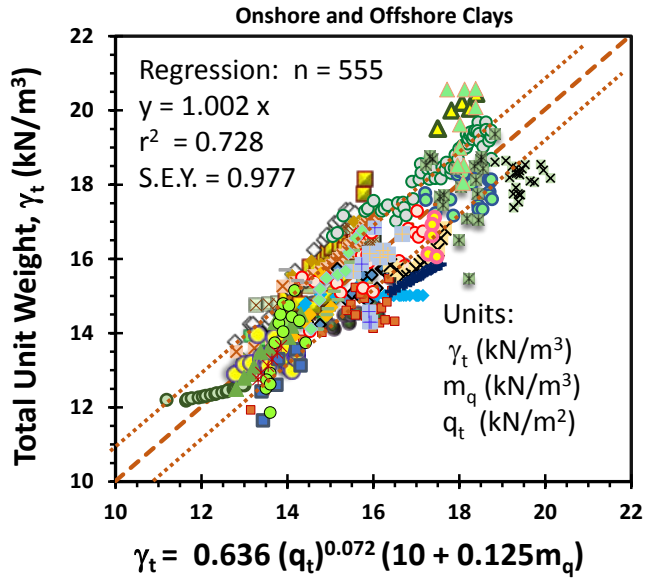

Figure 5. Soil unit weight of soft-firm clays from cone resistance (q_t) and resistance-depth ratio (m_q).

2.3 *Soil unit weight*

The use of normalized piezocone parameters requires the evaluation of total and effective overburden stresses ($\sigma_{vo}' = \sigma_{vo} - u_0$), where $\sigma_{vo} = \int \gamma_t \, dz$ and u_0 = hydrostatic porewater pressure. Therefore, an indirect assessment of unit weight (γ_t) is needed.

A general assessment of soil unit weight from CPT for a variety of soil types has been found related to the sleeve friction, as shown by Figure 4 (Mayne 2014):

$$\gamma_t/\gamma_w = 1.22 + 0.15 \cdot \ln (100*f_s/\sigma_{atm}+0.01) \qquad (6)$$

For soft-firm clays, the cone resistance exhibits a linear trend with depth that can be represented by the parameter $m_q = \Delta q_t/\Delta z$, termed the resistance-depth ratio. Two sets of regressions on q_t data both with and without an intercept (b = 0) giving similar slope values m_q are indicative of normally-consolidated (NC) to lightly-overconsolidated (LOC) clays (Mayne & Peuchen 2012). In contrast, different m_q slope values from the two regressions are characteristic of overconsolidated soils and thus the method is not applicable. It has been observed that the range of m_q in soft-firm clays generally occurs when the ratio $m_q < 80$ kN/m^3 (Mayne 2014).

For soft to firm clays, the resistance-depth ratio m_q gives an estimate of the average soil total unit weight over the depth of the deposit:

$$\gamma_t/\gamma_w = 1 + 0.125 \, m_q/\gamma_w \qquad (7)$$

It is interesting to note that the resistance-depth ratio has the same units as unit weight, thus can be employed as a normalizing parameter in the same manner that atmospheric pressure (σ_{atm}) is used for stress.

To capture variations in the unit weight with depth, a more elaborate trend is shown in Figure 5 in terms of q_t and m_q (Mayne & Peuchen 2012). This can be expressed in dimensionless form:

$$\gamma_t/\gamma_w = 0.886 \cdot (q_t/\sigma_{atm})^{0.072} \, [1 + 0.125 \cdot m_q/\gamma_w] \qquad (8)$$

2.4 *Unit weights at Bothkennar*

The estimating of soil unit weights from CPTu in soft clay are illustrated with a case study. For the Bothkennar site in Scotland, two sets of piezocone data were utilized from field testing by Nash et al. (1992a) and Powell & Lunne (2005), as presented in Figure 6. The agreement between the early sounding and later series is quite evident.

The evaluation of the m_q parameter is shown in Figure 7a, giving a value of the resistance-depth ratio: $m_q = 54$ kN/m^3. This can be input into equation (7) to give an estimated $\gamma_t = 16.7$ kN/m^3 which agrees well as an overall value when compared with lab unit weights obtained from Delft and piston type samples taken at the site that are shown in Figure 7b (Hight et al. 2003).

A slightly improved profile of estimated unit weight with depth is obtained using both the cone resistance q_t together with the m_q parameter, as seen by Figure 7b, per equation (8). Here, the profile of unit weight decreases slightly in the crust and then increases slightly with depth in the soft clay.

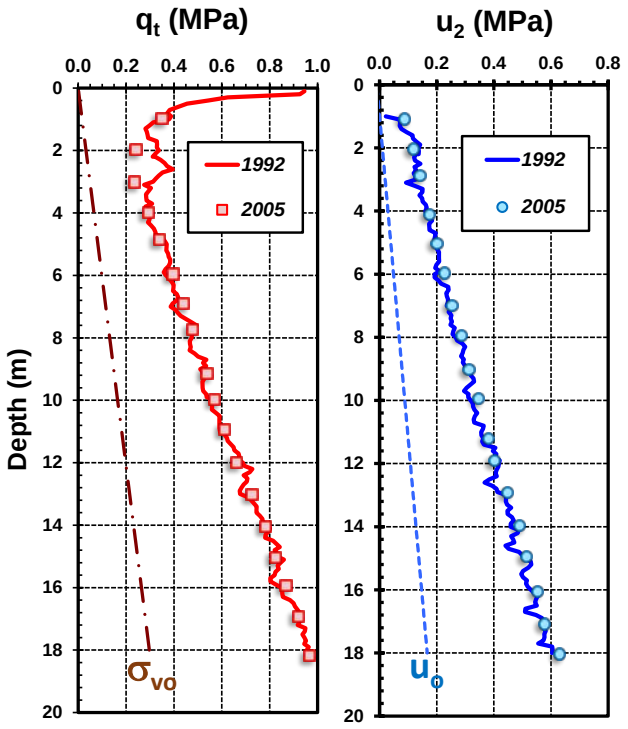

Figure 6. Results from two sets of piezocone sounding series at Bothkennar clay test site, UK (data from Nash et al. 1992 and Powell & Lunne 2005).

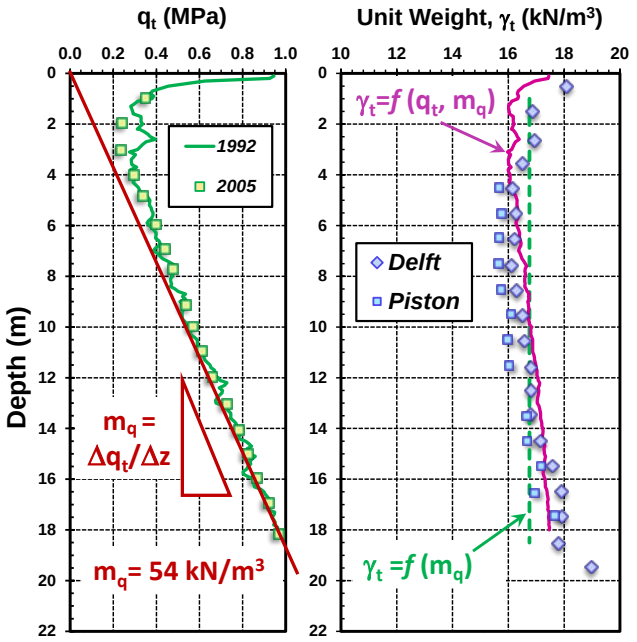

Figure 7. Bothkennar clay profiles showing: (a) evaluation of m_q ratio; (b) measured and estimated soil unit weights.

3 EFFECTIVE STRESS FRICTION ANGLE OF CLAY FROM PIEZOCONE

The prevailing shear strength of soils depends upon the frictional characteristics of soils, stress path, initial anisotropic state of stress, degree of drainage, direction of loading, and many other factors. Commonly, two extreme cases are sought for saturated geomaterials: (1) drained strength ($\Delta u = 0$) with corresponding effective stress friction angle (ϕ') and effective cohesion intercept (c'); and (2) undrained shear strength ($s_u = c_u$) corresponding to constant volume ($\Delta V/V_0 = 0$).

3.1 *Effective stress friction angle*

Since the piezocone takes measures of both total stress changes (q_t) and porewater pressures (u_2) during penetration into soil, the principle of effective stress can be realized (Sandven 1990). In the case of soft to firm clays, it can be taken that c' = 0 and the effective friction angle (ϕ') can be evaluated using the NTH (Norwegian Institute of Technology) solution detailed by Senneset et al. (1989) and Sandven & Watn (1995).

For the general case, undrained penetration is represented by:

$$q_{net} = (N_q - 1)\cdot(\sigma_{vo}' + a') - N_u \cdot \Delta u_2 \qquad (9)$$

where the attraction $a' = c'\cdot\cot\phi'$ and N_q = bearing capacity factor for end bearing or tip resistance is given by:

$$N_q = \tan^2(45°+\phi'/2)\cdot\exp[(\pi-2\beta)\cdot\tan\phi'] \qquad (10)$$

and β = angle of plastification which dictates the size of the failure zone. The term N_u is the bearing factor for porewater pressure (Senneset & Janbu 1985):

$$N_u = 6\cdot\tan\phi'\cdot(1+\tan\phi') \qquad (11)$$

Additional details are given by Sandven (1990) regarding the terms of attraction (a') and angle of plastification (β). The cone resistance number (N_m) is defined as:

$$N_m = \frac{q_t - \sigma_{vo}}{\sigma_{vo}' + c'\cdot\cot\phi'} = \frac{N_q - 1}{1 + N_u \cdot B_q} \qquad (12)$$

A discussion of evaluating the effective cohesion intercept c' is provided in a later section of this paper.

For the case when c' = 0, the parameter N_m is identical to the normalized cone resistance (Q) and the relationship becomes:

$$Q = \frac{N_q - 1}{1 + N_u \cdot B_q} = \frac{q_t - \sigma_{vo}}{\sigma_{vo}'} \qquad (13)$$

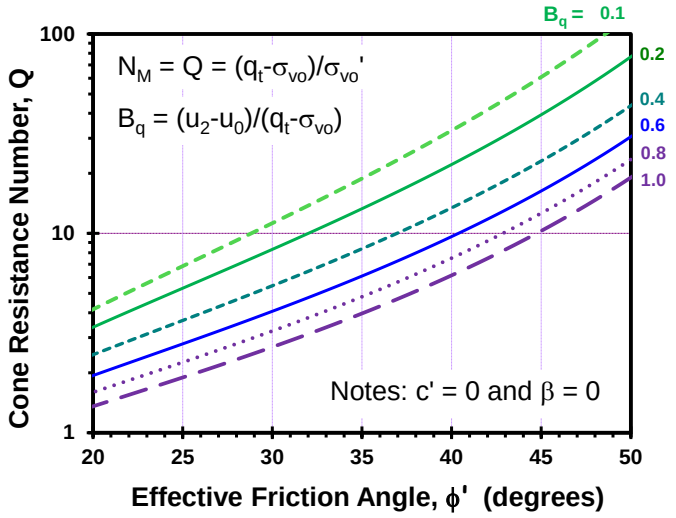

Figure 8. NTH graphical solution for ϕ' in terms of Q and B_q for simple case when c' = and β = 0.

Therefore, for the simplified case when β = 0 and c' = 0, the undrained limit plasticity solution relates Q to effective stress friction angle ϕ' and parameter B_q:

$$Q = \frac{\tan^2(45° + \phi'/2)\cdot\exp(\pi\cdot\tan\phi') - 1}{1 + 6\cdot\tan\phi'\cdot(1+\tan\phi')\cdot B_q} \qquad (14)$$

as presented graphically in Figure 8.

An approximate inversion of the NTH solution has been developed for individual values of Q and B_q for the case when c' = 0 and β = 0 (Mayne 2007):

$$\phi' = 29.5°\cdot B_q^{0.121}\cdot[0.256 + 0.336\cdot B_q + \log Q] \qquad (15)$$

This is applicable for the specific ranges of porewater pressure parameter ($0.1 < B_q < 1$) and effective stress friction angles ($20° < \phi' < 45°$).

3.2 *NTH application to Bothkennar CPTu data*

The NTH method is applied to the piezocone data from Bothkennar, Scotland (reported earlier in Figure 6). Figure 9 presents a plot of Δu_2 vs. q_{net} and gives regression best fit line slopes B_q = 0.62 and 0.65, respectively, for the 1992 and 2005 data sets.

Similarly, plots of q_{net} vs. σ_{vo}' are shown in Figure 10 and regression lines indicate $N_m = Q$ = 5.22 and 5.17, respectively. The regressions were completed using best fit line options with forced intercepts of zero, as the assumption here is that c' = 0. Using the paired values of Q and B_q input into Figure 8 give NTH-evaluated ϕ' = 32.9° and 33.3°, respectively.

Extensive laboratory programs and in-situ field tests of Bothkennar clay have been accomplished over the past three decades (Hight et al. 2003). These include many series of laboratory triaxials tests on both undisturbed and remolded samples taken by a variety of high quality samplers and different laboratories.

Results from a particular set produced by Allman & Atkinson (1992) are shown in Figure 11. These include several modes of shearing: triaxial compression (CK_0UC, CK_0DC) and extension (CK_0UE, CK_0DE) tests from both undrained and drained stress paths, all confirming that the characteristic ϕ' = 34° for Bothkennar clay.

Using the approximate expression for ϕ' = *fctn* (Q, B_q), Figure 12 presents the derived profiles of ϕ' with depth at Bothkennar using the two sets of CPTu data. These show good agreement with the summary ϕ' = 34° from the laboratory triaxial data, with slightly conservative evaluations by the CPTu approach.

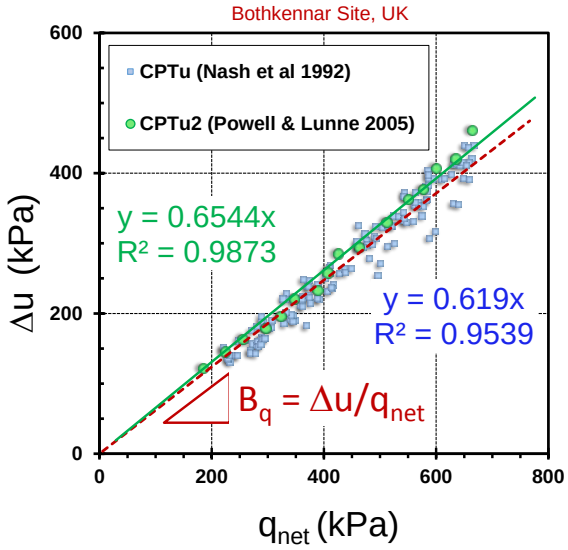

Figure 9. Plot of excess porewater pressure vs. net cone resistance from Bothkennar CPTu data.

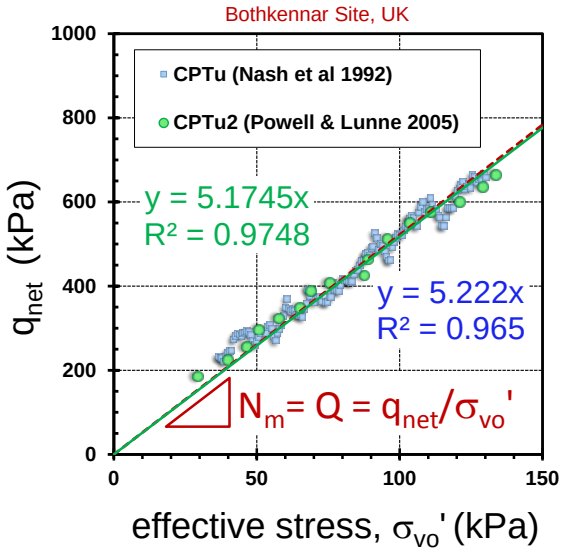

Figure 10. Plot of net cone resistance vs. effective overburden stress from Bothkennar CPTu data.

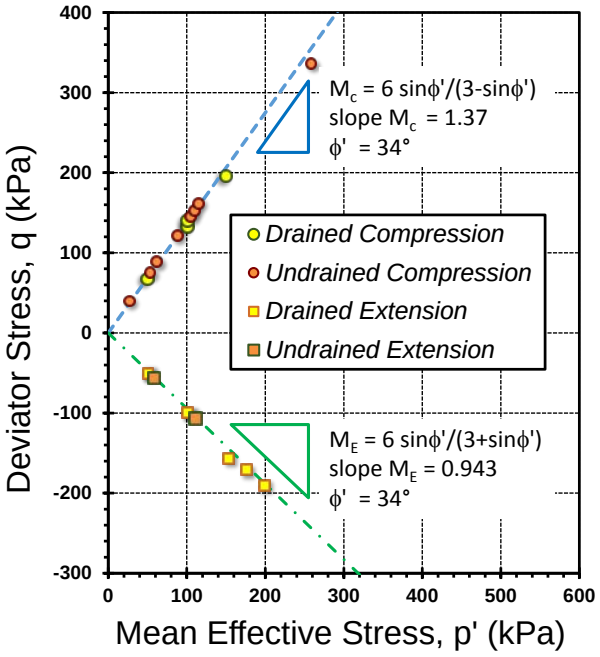

Figure 11. Results from triaxial tests on Bothkennar soft clay reported by Allman & Atkinson (1992).

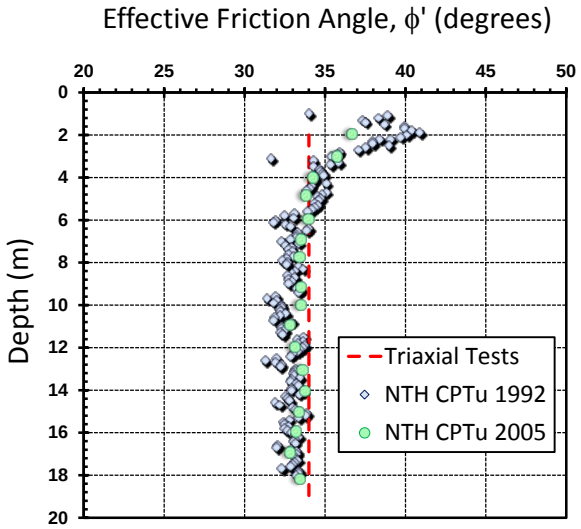

Figure 12. Profile of ϕ' at Bothkennar clay using CPTu Q and B_q and approximate NTH solution.

4 UNDRAINED STRENGTH PARAMETERS FROM PIEZOCONE

Undrained shear strength (s_u) is a total stress parameter measured at constant volume. The mode of shearing affects the magnitude of undrained shear strength in soft to firm clays. For instance, the Bothkennar clay has a family of s_u profiles that have been obtained from a variety of different lab and field tests. Figure 13 shows a relative sampling that show the hierarchy of s_u from highest to lowest: field vane tests (FVT), triaxial compression (TC), simple shear (SS), and triaxial extension (TE).

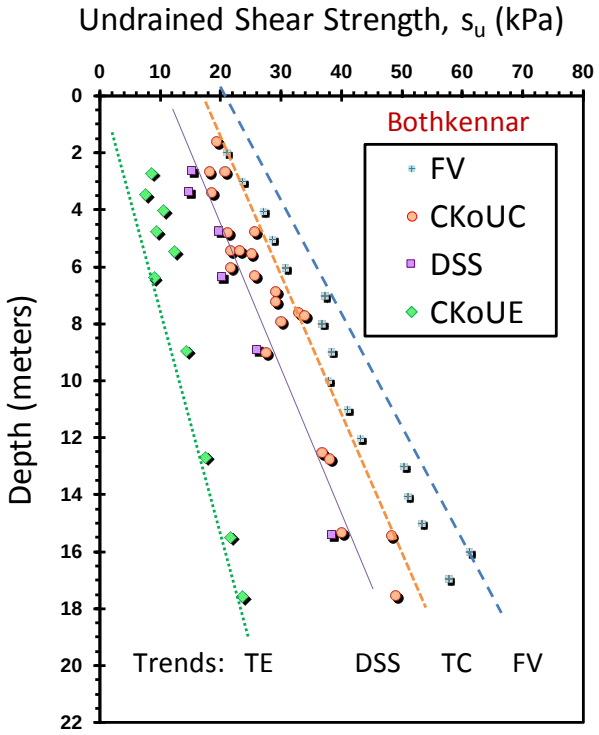

Figure 13. Family of s_u profiles for Bothkennar soft clay (data from Hight et al. 2003).

4.1 *Undrained shear strength from piezocone*

For CPT results, the undrained shear strength (s_u) is most often interpreted in terms of the net cone tip resistance. If the triaxial compression mode is taken as the relevant type of undrained shear strength (s_{uc}), then:

$$s_{uc} = \frac{q_{net}}{N_{kt}} \tag{16}$$

where N_{kt} = bearing factor for net tip resistance.

For CPTu in soft to firm clays, Lunne et al. (2005) recommend a value N_{kt} = 12 for s_{uc}. A study of piezocone data on 3 onshore and 11 offshore clays by Low et al. (2010) found the range: $8.6 \leq N_{kt} \leq 15.3$, with a mean value of N_{kt} = 11.9 for triaxial compression mode. Similarly, a larger study of 51 soft to firm intact clays found a mean value of N_{kt} = 11.8 for s_{uc} corresponding to the CAUC triaxial mode (Mayne et al. 2015).

For other shearing modes, other operational values of N_{kt} must be used. For instance, Low et al. (2010) found a mean N_{kt} = 13.6 for the lab average strength (s_{uAVE}) from triaxial compression, simple shear, and triaxial extension (range: $10.6 \leq N_{kt} \leq 17.4$), which is close to a simple shear mode (s_{uSS}). For calibration with the field vane (s_{uv}), they determined N_{kt} averages 13.3 with a range: $10.8 \leq N_{kt} \leq 19.9$.

Similarly, the undrained shear strength can be expressed in terms of the excess porewater pressures during penetration ($\Delta u = u_2 - u_0$):

$$s_{uc} = \frac{\Delta u}{N_{\Delta u}} \quad (17)$$

where $N_{\Delta u}$ = bearing factor for excess porewater pressures. For the triaxial compression mode, Lunne (2010) recommends a value of $N_{\Delta u} = 6$ for preliminary work or initial estimates until calibrated with laboratory tests on undisturbed samples. From their study, Low et al. (2010) indicate a mean value of $N_{\Delta u} = 5.88$, while the study by Mayne, Peuchen, & Baltoukas (2015) found a representative $N_{\Delta u} = 6.5$.

4.2 *Spherical cavity expansion*

For undrained shear, the spherical cavity expansion (SCE) solutions formulated by Vesic (1972, 1977) are interesting because they relate s_u to both q_{net} and excess porewater pressures (Δu):

$$N_{kt} = 4/3 \cdot [\ln(I_R) + 1] + \pi/2 + 1 \quad (18)$$

$$N_{\Delta u} = 4/3 \cdot \ln(I_R) \quad (19)$$

where $I_R = G/s_u$ = rigidity index and G = shear modulus. The rigidity index can also be considered as the reciprocal of a reference shear strain (γ_{ref}), thus $I_R = 1/\gamma_{ref}$. Adopting a characteristic shear strain at peak strength or failure of 1%, or $\gamma_{ref} = 0.01$, corresponds to an assumed default value of $I_R = 100$.

In truth, the shoulder position of excess porewater pressure measurements by piezocone (Δu_2) is comprised of two components: octahedral and shear-induced. For young to aged normally-consolidated clays with OCRs < 2, the shear induced portion is rather small compared to the octahedral portion (Baligh 1980; Burns & Mayne 2002). Therefore, as a first approximation to Δu in clays, SCE provides the octahedral component alone.

Since the undrained strength is given by:

$$s_{uc} = \frac{q_{net}}{N_{kt}} = \frac{\Delta u}{N_{\Delta u}} \quad (20)$$

It is noted that the parameter B_q interrelates the two bearing factors (Lunne 2010):

$$N_{\Delta u} = B_q \cdot N_{kt} \quad (21)$$

Therefore, spherical cavity expansion allows for a direct interrelationship between Δu_2 and q_{net} expressed simply as a function of rigidity index, as shown in Figure 14. In support of this notion, piezocone data from 34 soft-firm clay sites (Mayne & Peuchen 2012) are shown to validate the SCE relationships and the operational values of rigidity index are seen to fall within the range: $10 < I_R < 1000$. The data are separated into two groups comprised of 19 offshore clays and 15 onshore clay deposits.

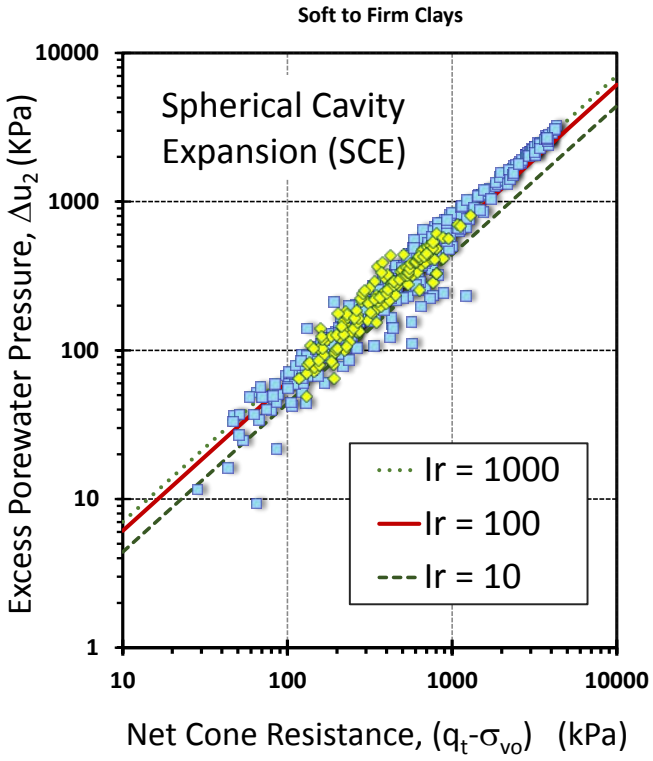

Figure 14. SCE relationship between Δu_2 and q_{net} with piezocone data from 15 onshore clays (yellow dots) and 19 offshore clays (blue dots).

Combining equations (18), (19), and (21), we find that rigidity index is simply a function of the porewater pressure parameter B_q:

$$I_R = \exp\left(\frac{2.93 \cdot B_q}{1 - B_q}\right) \quad (22)$$

For the data ranges shown in Figure 14, the operational range of $B_q = \Delta u/q_{net}$ varies from 0.45 to 0.75 with a central value of B_q of around 0.60. Statistical regression analyses on the onshore and offshore data gave mean B_q values of 0.62 and 0.69, respectively.

4.3 *SCE evaluated s_u from CPTu*

Substituting the SCE backfigured I_R back into the expressions for bearing factor terms, we obtain the following:

$$N_{kt} = \frac{3.90}{1 - B_q} \quad (23)$$

$$N_{\Delta u} = \frac{3.90}{(1/B_q)-1} \quad (24)$$

The SCE relationships between the bearing factors N_{kt} and $N_{\Delta u}$ with B_q are shown in Figure 15. Superimposed over these lines are the backfigured values from the study reported by Mayne, et al. (2015), with considerable scatter evident in the data.

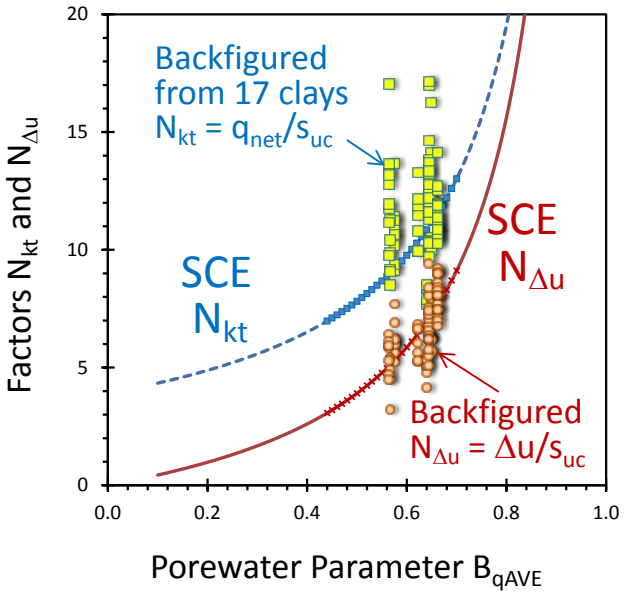

Figure 15. SCE relationships between cone bearing factors N_{kt} and $N_{\Delta u}$ with porewater parameter B_q. Data from piezocone tests and CAUC triaxial compression mode, s_{uc}.

In this endeavor, constant values of the bearing factors for any given clay are found using the average B_{qAVE} from the Δu vs. q_{net} plot. The SCE expressions can then be stated:

$$s_{uc} = \frac{q_{net}}{3.90} \cdot (1 - B_{qAVE}) \quad (25)$$

$$s_{uc} = \frac{\Delta u}{3.90} \cdot [(1/B_{qAVE}) - 1] \quad (26)$$

The application of the mean $B_{qAVE} = 0.65$ from the 2005 CPTu series of data for Bothkennar clay is used to provide assessments of s_{uc} profiles at the site based from both q_{net} and Δu, as shown in Figure 16. These are seen to be comparable, perhaps slightly high, when compared to the laboratory series of CAUC triaxial data from the site.

An alternative to the above approach is to utilize the specific B_q value at each elevation to drive the SCE solutions for the N_{kt} and $N_{\Delta u}$ factors, thus both variables with depth. In this case, both the q_{net} and Δu readings give the same exact profile of s_{uc}. In fact, the direct solution for s_u is given simply as:

[13] $$s_{uc} = \frac{q_t - u_2 - \sigma_{vo}'}{3.90} \quad (27)$$

Using this approach, the derived profiles of s_{uc} for both the 1992 and 2005 soundings are shown in Figure 17. The 1992 sounding was digitized in more detail at approximate 0.1-m intervals, while the 2005 sounding was digitized at coarser 1-m intervals as a check to verify the quality of the earlier CPTu data. Thus, while this approach also gives relatively reasonable agreement with both the lab triaxial compression results and field vane data, the resulting profiles shows more variability and skittishness at any given elevation, specifically the finer data from 1992 vintage.

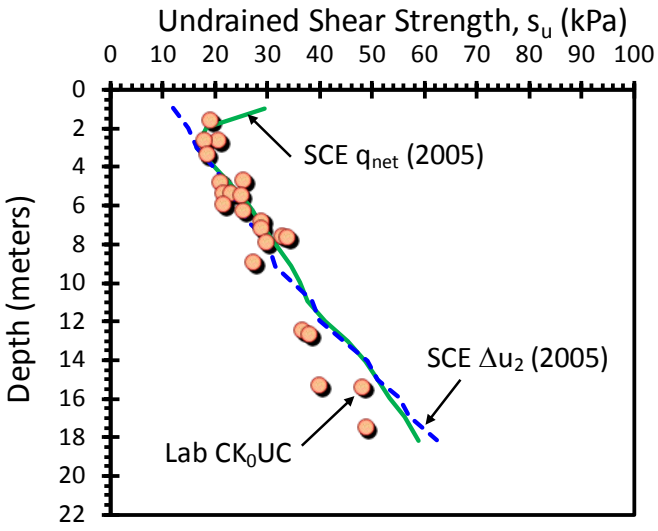

Figure 16. Profiles of s_{uc} at Bothkennar using SCE solutions for q_{net} and Δu with the average value of B_q.

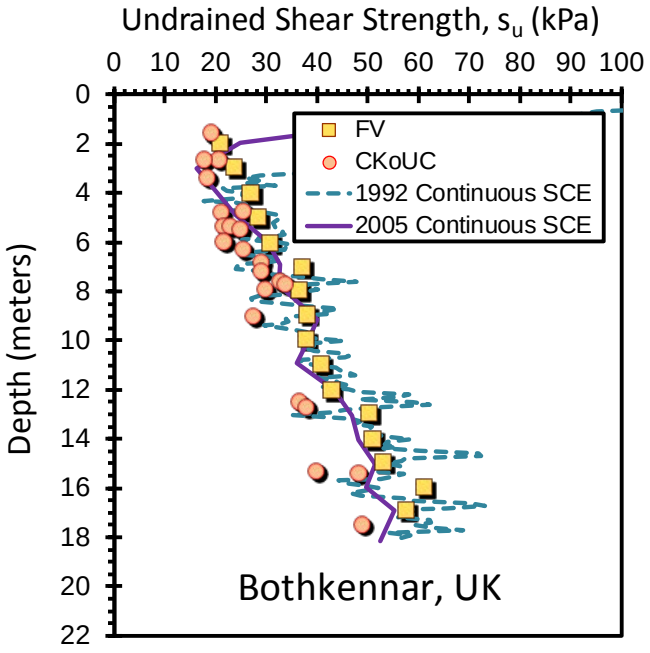

Figure 17. Profiles of undrained shear strength at Bothkennar using continuous B_q data.

4.4. *Strength from effective cone resistance*

Another option for assessing s_u in clays is via the effective cone resistance (Lunne et al. 1997):

$$s_u = \frac{q_t - u_2}{N_{ke}} \quad (28)$$

where N_{ke} is a bearing factor averaging about 8.0 in soft-firm clays (Mayne et al. 2015). Yet in consideration of SCE theory alone per equation (27), this relationship cannot be expressed in this form.

In the case of a hybrid SCE model with critical state soil mechanics (CSSM), however, it can be expressed in terms of effective cone resistance where the bearing term for CIUC triaxial is found as (Chen & Mayne 1993):

$$N_{ke} = 2/M_c + 3.90 \quad (29)$$

where M_c = q-p' frictional parameter for triaxial compression as shown in Figure 11.

5 EFFECTIVE STRESS STRENGTH PARAMETERS OF CLAY FROM DMT

5.1 *Equivalent porewater pressures from DMT*

The contact pressures (p_0) from DMT readings in clays appear to be dominated by the porewater pressures induced during blade insertion (Mayne 2006). For soft to firm intact clays, the assertion can be made that:

$$\Delta u = p_0 - u_0 \quad (30)$$

which allows for the net contact pressure to be expressed in terms of SCE:

$$p_0 - u_0 = 4/3 \cdot s_u \cdot \ln(I_R) \quad (31)$$

5.2 *Cavity expansion link for DMT*

Spherical cavity expansion also expresses the magnitude of change in horizontal stress for probes pushed into clay:

$$\Delta\sigma_h = 4/3 \cdot s_u \cdot (\ln I_R + 1) \quad (32)$$

As a first approximation, the net expansion pressure from the flat dilatometer can be considered as a measure of this horizontal stress change:

$$\Delta\sigma_h = p_1 - u_0 \quad (33)$$

From (16) and (18), the net cone resistance is expressed directly from SCE as:

$$q_{net} = 4/3 \cdot s_u \cdot (\ln I_R + 1) + \pi/2 + 1 \quad (34)$$

and by combining equations (31) through (34), an equivalent net cone resistance can be found in terms of the dilatometer pressures:

$$q_{net} = 2.93 \cdot p_1 - 1.93 \cdot p_0 - u_0 \quad (35)$$

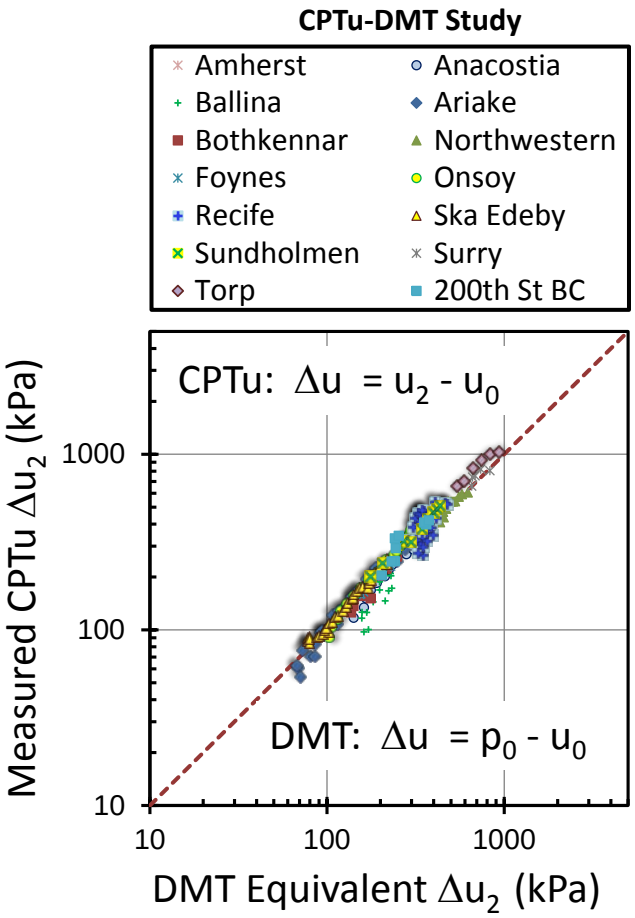

Figure 18. Measured CPTu Δu_2 versus DMT-equivalent excess porewater pressure: $\Delta u = p_0 - u_0$.

5.3 *CPTu-DMT database in clays*

An in-situ database of 12 clays that were subjected to both piezocone and flat dilatometer tests was compiled to validate the CPTu-DMT interrelationships. Figure 18 shows the measured excess porewater pressures (Δu_2) from piezocone tests vs. the equivalent Δu calculated from flat plate dilatometer tests according to equation (31). These are seen to be quite comparable and the results are consistent with the earlier observations by Mayne & Bachus (1989) for a variety of clays.

Similarly, Figure 19 shows the net cone resistance ($q_{net} = q_t - \sigma_{vo}$) from CPTu soundings at the same elevations in the same clays are plotted vs. the equivalent q_{net} obtained from DMT readings per equation (35). Again, the results are comparable.

5.4 *Equivalent NTH method for DMT*

These findings allow for the application of the NTH undrained limit plasticity solution to flat dilatometer tests in clays in assessing the effective stress friction angle (ϕ'). In particular, the tentative use would be restricted to soft-firm NC-LOC clays where $c' = 0$ is a common assumption. As noted previously for the CPTu, two options are available for obtaining ϕ' using the NTH solution: (1) individual plots of q_{netDMT} vs. σ_{vo}' to obtain N_m and Δu_{DMT} vs. q_{netDMT} to obtain B_{qDMT}; and (2) approximate ϕ' expression using equivalent Q_{DMT} and B_{qDMT} which are given by:

$$Q_{DMT} = \frac{2.93 \cdot p_1 - 1.93 \cdot p_0 - u_0}{\sigma_{vo}'} \qquad (34)$$

$$B_q = \frac{p_0 - u_0}{2.93 \cdot p_1 - 1.93 \cdot p_0 - u_0} \qquad (35)$$

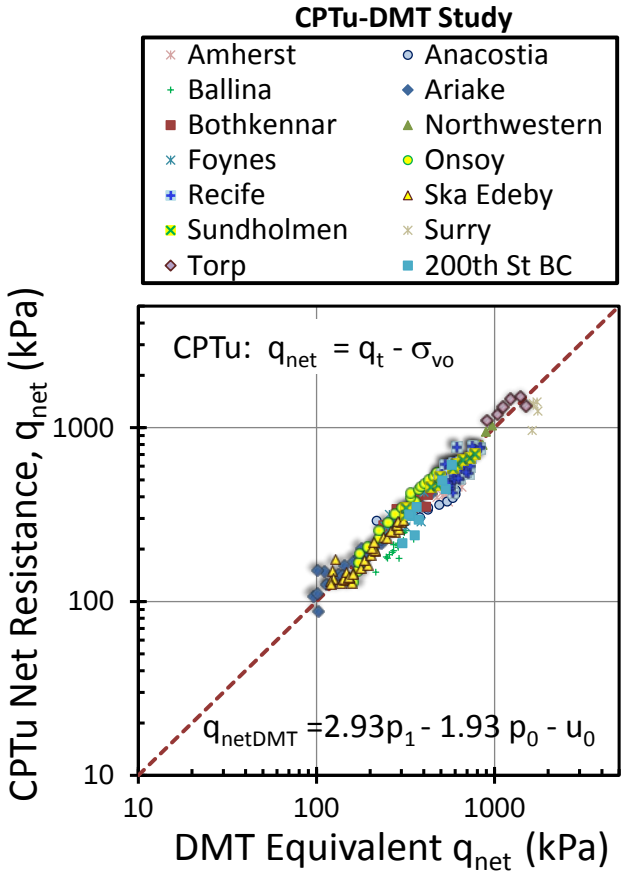

Figure 19. Measured CPTu q_{net} versus DMT-equivalent net cone resistance: q_{net}.

5.5 *Application to Bothkennar DMT data*

The results of a representative DMT sounding at the Bothkennar soft clay site are reported by Hight et al. (2003) and shown in Figure 20 with the associated DMT material index (I_D) profile. The p_0 and p_1 readings are seen to increase approximately linearly with depth with the contact pressures ranging from 137 to 500 kPa and the expansion pressures varying from 175 to 600 kPa in the depth range from 2 m to 16 m. Groundwater is approximately 1 m deep.

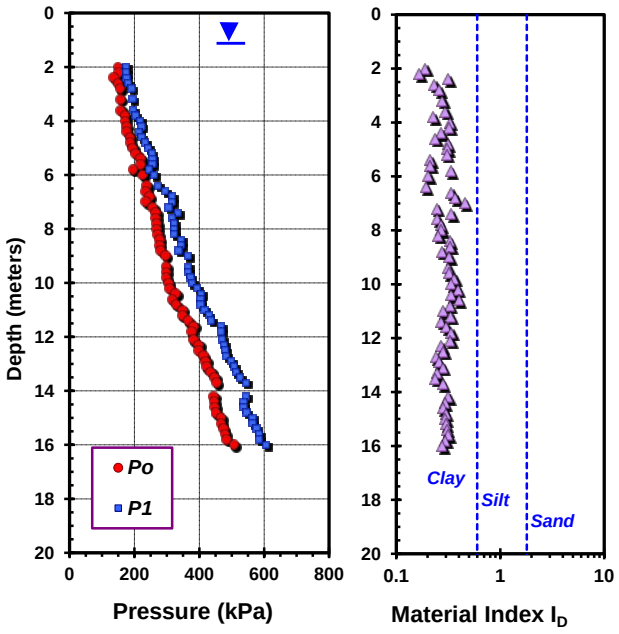

Figure 20. Representative DMT sounding at Bothkennar clay site (data from Hight et al. 2003).

The post-processing of equivalent Δu vs q_{net} is presented in Figure 21, giving an equivalent $B_{qDMT} = 0.54$. Similarly, the plotting of equivalent q_{netDMT} vs. effective overburden stress in Figure 22 gives a slope where $N_m = Q = 5.64$. Using either Figure 8 or equation (14) with these values gives an operational friction angle $\phi' = 32.6°$. Referring once more to Figure 11 that hosts the effective stress strength envelope for undrained and drained triaxial compression and extension test results on Bothkennar clay (Allman & Atkinson 1992), the characteristic $\phi' = 34°$ from the laboratory series is seen to be in general agreement with the in-situ evaluations.

Alternatively, the approximate NTH solution using derived profiles of Q_{DMT} and B_{qDMT} per equations (34) and (35) are presented in Figure 23a. These can be processed at all elevations using equation (15) to produce a profile of ϕ' with depth, indicating a range $32° < \phi' < 35°$ in the depth range of 4 to 16 m.

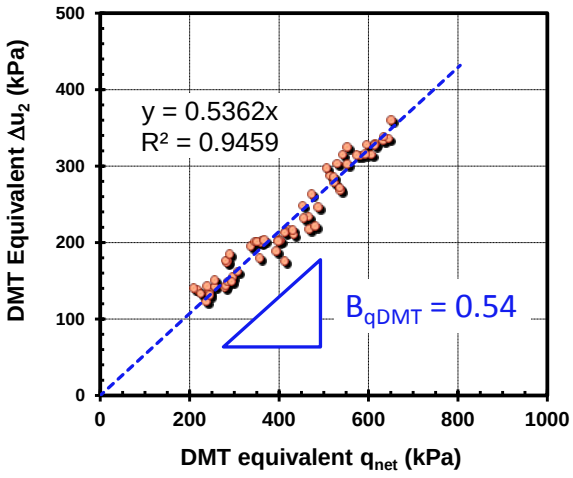

Figure 21. Post-processing DMT data to obtain equivalent B_q parameter at Bothkennar.

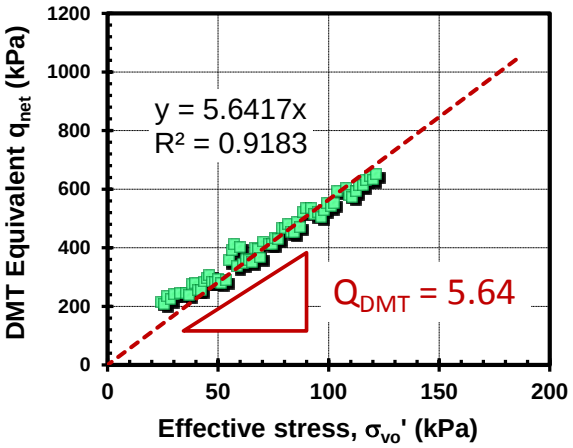

Figure 22. Post-processing to obtain DMT-equivalent Q in Bothkennar soft clay.

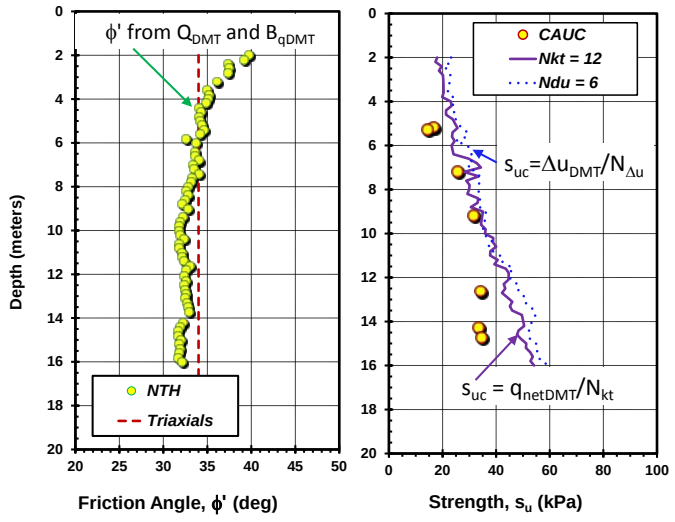

(a) (b)

Figure 23. Profiles at Bothkennar: (a) ϕ' from approximate NTH solution using Q_{DMT} and B_{qDMT}; (b) shear strength in triaxial compression (s_{uc}) using q_{netDMT} and Δu_{DMT}

Of additional note, the equivalent profiles of q_{netDMT} and Δu_{DMT} can be used with the classical N_{kt} = 12 and $N_{\Delta u}$ = 6 approach given by equations (16) and (17) to evaluate the undrained shear strengths, as presented in Figure 23b. These are seen to be somewhat comparable with lab TC tests on undisturbed samples for depths < 12 m but do appear to overpredict s_{uc} at greater depths.

6 EFFECTIVE STRESS COHESION INTERCEPT

6.1 *NTH Solution for c'*

The NTH solution can also provide an evaluation of both Mohr-Coulomb parameters: c' and ϕ'. In the general case, the cone resistance number given by equation (12) is expressed:

$$N_m = \frac{\tan^2(45° + \frac{1}{2}\phi') \cdot \exp[(\pi - 2\beta) \cdot \tan\phi'] - 1}{1 + 6 \cdot \tan\phi' \cdot (1 + \tan\phi') \cdot B_q} \quad (36)$$

When plotting q_{net} vs. σ_{vo}' to obtain the slope N_m, a negative intercept on the σ_{vo}' axis is the value of attraction a' = c'·cotϕ'. An approximate inversion of (36) to give ϕ' directly from N_m, β, and B_q can be formulated as:

$$\phi' \approx 30° \cdot 10^{0.0035\beta} \cdot B_q^{0.121} \cdot [0.256 + 0.336 \cdot B_q + \log N_m] \quad (37)$$

which is valid for the following parametric ranges: 20° ≤ ϕ' ≤ 40°, -30° ≤ β ≤ +20°, and 0.1 ≤ B_q ≤ 1.0. The evaluation of c' from CPTu data in clays is best illustrated by an example, as provided subsequently.

6.2 *Effective cohesion intercept of Bothkennar clay*

The critical state line (CSL) for Bothkennar clay was shown in Figure 11 as adequately represented by ϕ' = 34° and c' = 0. These values correspond to triaxial tests performed on reconstituted specimens of the clay, as well as to triaxial compression tests on undisturbed clay when evaluated at q_{max}. For a failure envelope taken at larger strains, or for overconsolidated states, it is possible to assign an apparent cohesion intercept value.

Post-processing the two sets of CPTu results from Bothkennar (1992 series and 2005 series) are shown in Figure 24, in this case allowing a general linear expression with both slope (m) and intercept (b). This is in contrast to the same data presented earlier in Figure 10 where the linear trend was forced

through the origin. The slope of q_{net} versus σ_{vo}' plotting averages N_m = 4.68. The ratio of the slope (m) to the ordinate axis intercept (b) gives the attraction (a') which is the negative intercept on the abscissa axis: a' = m/b. For Bothkennar, the average a' = 10.3 kPa. The corresponding B_q parameter remains unchanged, as per Figure 9, and averages B_q = 0.64. Adopting $\beta = 0°$, the inverted NTH solution gives the following Mohr-Coulomb effective stress strength parameters: $\phi' = 31.7°$ and c' = 6.4 kPa.

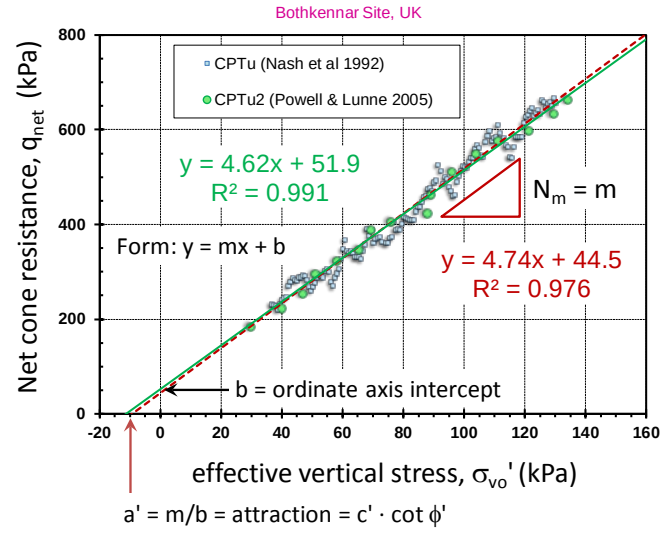

Figure 24. Evaluation of N_m and attraction a' in Bothkennar clay (alternate CPTu post-processing to that in Figure 10).

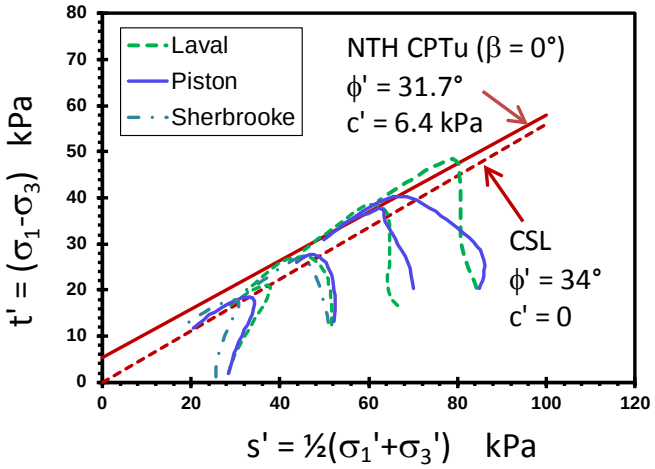

Figure 25. Triaxial stress paths for undisturbed Bothkennar clay (data from Hight et al. 1992) and superimposed c'-ϕ' derived parameters from NTH CPTu analyses.

These c'-ϕ' parameters are compared to CAUC triaxial tests on undisturbed specimens of Bothkennar clay in Figure 25. The CAUC tests include three separate series from high-quality sampling at the national test site using Laval, piston, and Sherbrooke type samplers (Hight et al. 1992). The CSL frictional characteristics represented by c' = 0 and $\phi' = 34°$ are shown for reference (Allman & Atkinson 1992). On the t-s' plot, these correspond to a slope angle $\alpha = 29.2°$ and intercept $a^* = c'\cdot\cos\phi' = 0$. Superimposed over the individual stress paths are the NTH CPTu-derived parameters ($\phi' = 31.7°$ and c' = 6.4 kPa). Here, the corresponding t-s' parameters are given as: angle $\alpha = 27.7°$ and intercept $a^* = c'\cdot\cos\phi' = 5.4$ kPa. Overall, the agreement between the Mohr-Coulomb envelope and laboratory triaxial data is reasonable.

6.3 *Alternative relationships for c'*

Notably, c' = 0 is a common assumption for soft to firm clays with OCRs < 2. Nevertheless, some stability analyses involving natural slopes, excavations, and soil nail walls require an assessment of c' for limit equilibrium and/or finite element studies. Also, overconsolidated soils may show an apparent cohesion intercept and friction angle.

Guidance on the selection and magnitude of c' can be found in a few other sources. Mayne & Stewart (1988) review data from CIUC and CAUC triaxial data on 16 different NC to OC clays and conclude that the effective cohesion intercept relates to the effective preconsolidation stress, expressed as the ratio c'/σ_p':

$$0.03 < c'/\sigma_p' < 0.06 \qquad (38)$$

Mesri & Abdel-Ghaffar (1993) review 60 slope failures in clays and backfigure strength parameters from stability analyses finding that:

$$0.003 < c'/\sigma_p' < 0.11 \qquad (39)$$

Sorensen & Okkel (2013) report that a common guideline in Scandinavia is that:

$$c' \approx 0.1\, s_u \qquad (40)$$

A simplified approach to undrained strength assessment for embankment stability analyses on soft clays is well documented (Jamiolkowski et al. 1985) and more recently confirmed for offshore applications (DeGroot et al. 2011):

$$\text{DSS: } s_u = 0.23\, \sigma_p' \qquad (41a)$$

$$\text{TC: } s_u = 0.29\, \sigma_p' \qquad (41b)$$

Thus combining (40) with (41b) indicates:

$$c' \approx 0.03\, \sigma_p' \qquad (42)$$

which is consistent with the aforementioned triaxial trends given by equation (38) and backfigured slope stability strength parameters given by (39).

In fact, for uncemented clays and silts, especially those that are NC-LOC, the effective cohesion intercept (c') is a pseudo-parameter as it appears to be an extrapolated value from the yield surface when force-fitting a linear expression for strength (i.e., Mohr-Coulomb envelope: $t_{max} = c' + \sigma' \cdot \tan\phi'$). A generalized yield surface is shown in Figure 26 in terms of Cambridge q-p' space with the CSL. That portion of the curved yield surface that extends above the CSL in the OC region can be extended back to an intercept on the ordinate axis, giving an apparent effective intercept: $q_c' = 2c' \cdot \cot\phi' \cdot M_c$.

For the Bothkennar clay, Hight et al. (2003) present the results of the interpreted yield surface from stress path testing, as shown on Figure 27. Here, the axes are normalized to the corresponding preconsolidation stress (σ_p') to account for the various sampling depths and the fact that σ_p' generally increases with depth.

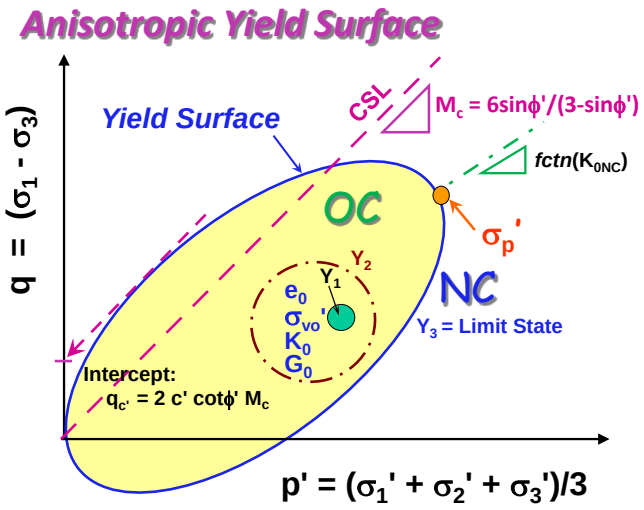

Figure 26. Generalized yield surface in q-p' space with projected intercept giving an apparent effective cohesion intercept.

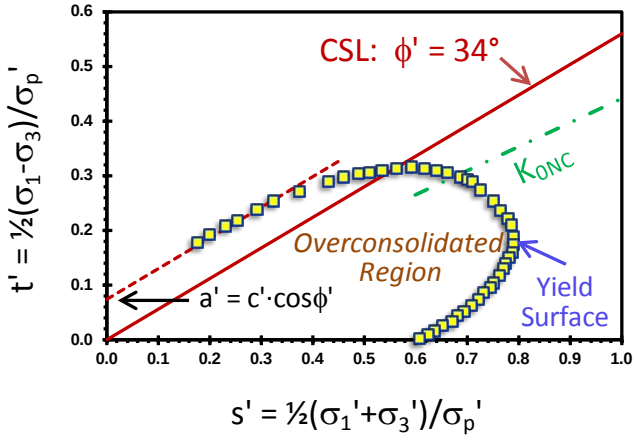

Figure 27. Yield surface for Bothkennar clay in t-s' space.

Thus, one outstanding question relates to the applicable value of σ_p' for normalization of the derived c' from the NTH solution on CPTu and/or DMT soundings, since the analysis of data is performed over the entire depth of the sounding. One possibility is to use the value of σ_p' at an effective stress equal to one atmosphere: $\sigma_{vo}' = \sigma_{atm}$, while another might consider use of the overconsolidation difference: $OCD = (\sigma_p' - \sigma_{vo}')/\sigma_{atm}$. However, the OCD really pertains to soils that are mechanically prestressed, such as removal of overburden by erosion, glaciation, or excavation (Locat et al. 2003). For some NC-LOC clays, there has been erosion but perhaps most of the observed preconsolidation has been due to other mechanisms such as secondary compression and ageing, groundwater fluctuations, diagenesis, and/or other factors.

7 STRESS HISTORY

In-situ tests are often used to give an initial first look at the stress history of clay deposits, as well as to supplement the more definitive results of one-dimensional consolidation tests on high-quality specimens. The CPT and DMT are particularly advantageous in this regard because they collect data at frequent depth intervals of 20 and 200 mm, respectively, whereas other tests (e.g., VST, PMT) provide readings on the order of 1 to 1.5 m intervals.

The CPT and DMT data in clays can be interpreted using empirical methods (e.g., Larsson & Åhnberg 2005), analytical approaches (e.g., Konrad & Law 1987; Mayne 2001, 2007), and/or numerical solutions (Yu & Mitchell 1998; Finno 1993). Herein, the simple SCE solutions will be applied to soft to firm NC-LOC clays.

7.1 *SCE solution for OCR from CPTu*

Critical state soil mechanics (CSSM) provides a link between undrained shear strength and stress history in terms of overconsolidation ratio: $OCR = \sigma_p'/\sigma_{vo}'$, where σ_p' = preconsolidation stress or effective yield stress. For the case of triaxial shearing of isotropically consolidated specimens (CIUC):

$$s_{uc} = \left(\frac{M_c}{2}\right)\left(\frac{OCR}{2}\right)^{\Lambda} \sigma_{vo}' \qquad (43)$$

where $\Lambda = 1 - C_s/C_c$ = plastic volumetric strain ratio, C_s = swelling index, and C_c = virgin compression index. For most clays and silts, the value of Λ is

about 0.8 to 0.9 (Jamiolkowski et al. 1985; Larson & Åhnberg 2005). Combining (16), (18), and (43) yields an expression for OCR in terms of normalized cone resistance: Q = qnet/svo' (Mayne 1991):

$$OCR = 2 \cdot \left[\frac{Q}{M_c \cdot \{\tfrac{2}{3} \cdot (1 + \ln I_R) + \tfrac{\pi}{2} + \tfrac{1}{2}\}} \right]^{1/\Lambda} \qquad (44)$$

Similarly, an expression can be found in terms of normalized excess porewater pressure:

$$OCR = 2 \cdot \left[\frac{\Delta u / \sigma_{vo}'}{\tfrac{2}{3} \cdot M_c \cdot \ln I_R} \right]^{1/\Lambda} \qquad (45)$$

As a first approximation, the power law formats can be removed by assuming that $\Lambda = 1$. Then, the expression in (44) can be reduced to provide a direct evaluation of the preconsolidation stress in terms of net cone resistance:

$$\sigma_p' \approx \frac{q_{net}}{M_c \cdot (1 + \tfrac{1}{3} \ln I_R)} \qquad (46)$$

Similarly, equation (45) is reduced to relate the yield stress in terms of excess porewater pressure:

$$\sigma_p' \approx \frac{\Delta u}{\tfrac{1}{3} M_c \cdot \ln I_R} \qquad (47)$$

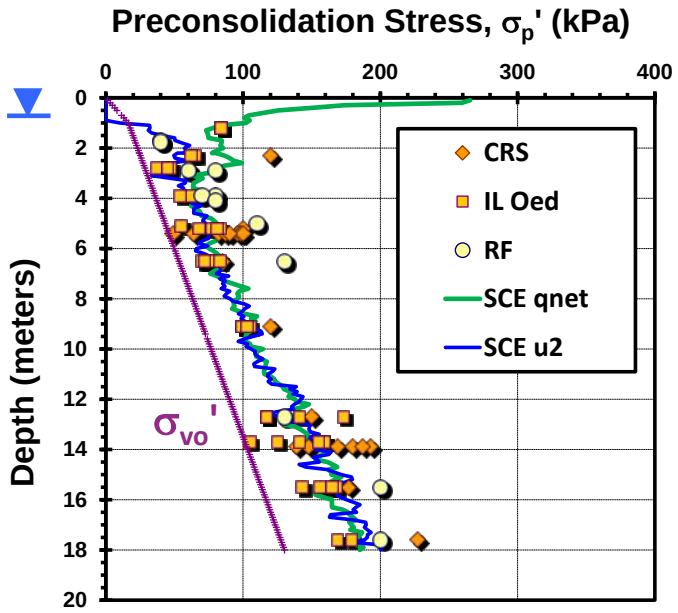

Figure 28. SCE-CPTu estimated and laboratory measured profiles of σ_p' at Bothkennar soft clay site.

7.2 *Application of SCE-CPTu-OCR to Bothkennar*

The SCE solutions for stress history evaluation can be applied to the Bothkennar CPTu data. All parameters are found from the post-processing of the sounding results. The value of $M_c = 1.37$ is found from the CSL $\phi' = 34°$ using the NTH effective penetration theory, as detailed earlier in Section 3.2. An operational value of rigidity index (I_R) is determined from the average B_q using equation (22). The overall $B_q = 0.619$ provides $I_R = 116$ for the CPTu reported by Nash et al. (1992a).

Consequently, for the Bothkennar clay, the SCE expressions become simply: $\sigma_p' = 0.28\ q_{net}$ and $\sigma_p' = 0.46\ \Delta u_2$. In Figure 28, these two CPT profiles are compared with three series of consolidation tests available from an extensive laboratory testing program conducted for the site (Nash et al. 1992b). One-dimensional consolidation tests included: (a) incremental-load type by Bristol University; (b) constant-rate-of-strain (CRS) types by Bristol Polytechnic; and (c) restricted flow (RF) tests at Oxford University. It can be seen that the piezocone profiles derived from q_{net} and Δu readings give very good agreement with the laboratory reference values.

7.3 *SCE solution for OCR from DMT*

Using the SCE link established in Section 5, a companion set of analytical solutions can be established for the flat dilatometer test in clays. For the net resistance relationships given by (44) and (46), the equivalent simplified expression for the DMT becomes:

$$\sigma_p' \approx \frac{2.93 p_1 - 1.93 p_0 - u_0}{M_c \cdot (1 + \tfrac{1}{3} \ln I_R)} \qquad (48)$$

For the second case where $p_0 \approx u_2$, then equations (45) and (47) provide the relationship:

$$\sigma_p' \approx \frac{p_0 - u_0}{\tfrac{1}{3} M_c \cdot \ln I_R} \qquad (49)$$

7.4 *Application of SCE-DMT-OCR to Bothkennar*

The SCE solutions for stress history from DMT readings can be applied to the Bothkennar data set. Again, the $M_c = 1.37$ is found from the CSL $\phi' = 34°$ characteristic value. The post-processing of the Δu_{DMT} vs. q_{netDMT} in Figure 21 gives an equivalent $B_{qDMT} = 0.54$. From equation (22), the backfigured $I_R = 31$ which seems a bit lower than the CPTu-

estimated value of 116. Luckily, the results are not highly sensitive the value of I_R.

A comparison of the two DMT profiles for σ_p' are presented with the three series of laboratory consolidometer tests in Figure 29. It is evident that the DMT estimates are on the high side of the results, perhaps because of the underestimation of the operational I_R value. Also shown for comparison is the conventional interpretation of OCR from the K_D parameter given by Marchetti (1980). This too matches toward the high side when compared with the lab benchmark values.

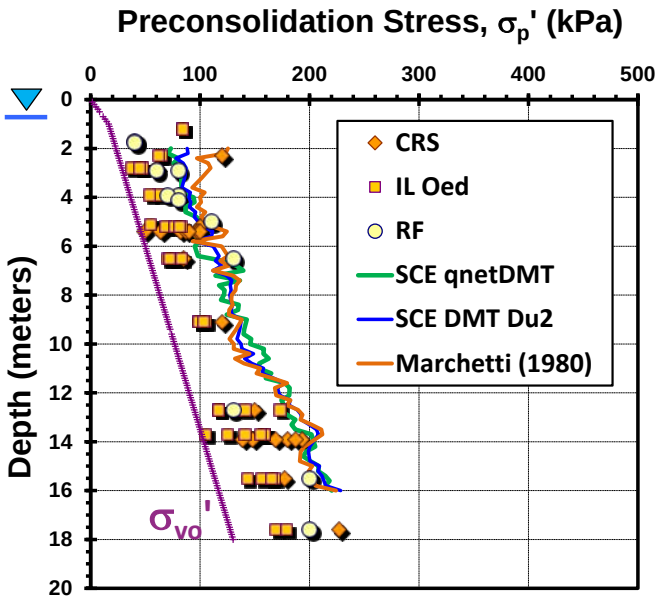

Figure 29. SCE-DMT estimated and laboratory measured profiles of σ_p' at Bothkennar soft clay site.

8 CALIBRATION OF NTH METHOD FOR CPTU

8.1 *Effective friction angles of clays*

A good number of natural clays have effective stress friction angles that are around 30°, as measured by triaxial compression tests. A review of effective frictional envelopes and yield surfaces of 50 worldwide deposits by Diaz-Rodriguez, et al. (1992) showed the full range: 17.5° < ϕ' < 43° for natural clays. A recent statistical review of measured ϕ' from 453 different clays (Mayne 2012, 2013) found that the mean and standard deviations averages ϕ' = 28.61° ± 5.05° when determined using triaxial compression tests (CAUC and CIUC).

For several natural Norwegian clays, Sandven (1990) calibrated the NTH CPTu solution with effective friction angles measured by triaxial compression tests on undisturbed samples, with values of ϕ' in the general ranges as noted above.

8.2. *Clay chamber tests*

A study of data from mini-piezocone penetrometers in calibration chamber tests found that the NTH gave good predictions for prepared deposits of clays, mostly having used kaolin and/or kaolinite-sand mixtures in the testing programs (Ouyang et al. 2016). Chamber test results from mini-CPTu series performed at one research group (Swedish Geotechnical Institute) and 8 universities were compiled for review (Cornell, Cambridge, LSU, Purdue, Oxford, Sheffield, Sangmyung, University of Western Australia). An interesting aspect of kaolinitic clays is that the clay mineral has a rather low friction angle (20° < ϕ' < 23°), whereas when mixed with sands and/or fine silica, a higher frictional characteristic is observed: 30° < ϕ' < 33°, similar to natural clays, as discussed by Rossato et al. (1992).

A comparison of triaxial-measured versus CPTu-calculated ϕ' using the NTH solution is presented in Figure 30. Kaolinite and kaolin-mixtures predominate here and are shown by circles. Results from Bothkennar clay (Section 3.2), are also shown, albeit its mineralogy is primarily illite with additional constituents of quartz, feldspar, mica, chlorite, and kaolinite. Overall, very good agreement is noted for this dataset. Note also that an improved estimate (close to 1:1 line) is made if the assumed β = - 5°.

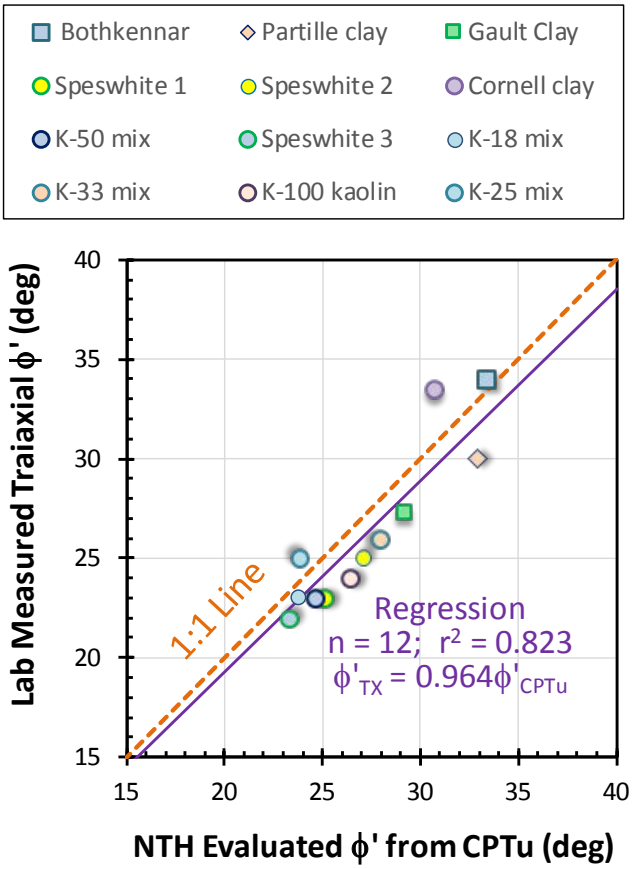

Figure 30. Calibration of NTH CPTu solution using data from clay calibration chamber tests (data from Ouyang et al. 2016).

9 DRAINAGE CONSIDERATIONS

9.1 *Drained versus undrained*

The concepts of drained vs. undrained behavior have been clarified through the framework of critical state soil mechanics and indicate that an infinite number of stress paths may lie in between these two extreme condidtions (Schofield & Wroth, 1968; Wood 1990; Mayne et al. 2009; Holtz et al. 2011). These notions have recently been examined experimentally by the introduction of in-situ twitch testing, whereby the rate of the test is varied to assess drainage characteristics and/or strain rate effects (Randolph 2004). Twitch testing has been accomplished using CPT and CPTu, T-bar, ball penetrometers, and vanes.

9.2 *Centrifuge CPT twitch tests in kaolin*

A series of CPTu twitch tests in centrifuge deposits of normally-consolidated kaolin clay are reported by Schneider et al. (2007). A mini-piezocone of diameter d = 10 mm was used in tests at accelerations of 160 g. The CPT velocity (v) was varied from 3 mm/s to 0.0004 mm/s and the recorded responses in measured q_t and u_2 were used to prepare Figures 31 and 32. A normalized velocity is defined as:

$$V = v \cdot d/c_v \qquad (50)$$

where v = probe velocity, d = probe diameter, and c_v = coefficient of consolidation. For the NC kaolin, the reported values: $0.060 < c_v < 0.076$ mm^2/s.

DeJong et al. (2013) have reported that essentially undrained behavior occurs when V > 30, while drained behavior with low porewater pressure response ($B_q < 0.1$) is observed when V < 0.3. These thresholds generally appear valid for the kaolin CPTu tests shown, albeit perhaps a slightly higher V limit for the undrained domain. The intermediate values of V correspond to partially drained or partly undrained conditions.

The changes in cone tip resistance with penetration rate can be represented in terms of normalized cone resistance (Q) and an algorithm suggested by DeJong et al. (2013):

$$\frac{Q}{Q_{ref}} \approx 1 + \left(\frac{(Q_{drained}/Q_{ref}) - 1}{1 + (V/V_{50})^c} \right) \qquad (51)$$

where $Q = q_{net}/\sigma_{vo}'$, $Q_{drained}$ is the normalized cone resistance for fully drained penetration (i.e., when $B_q = 0$), Q_{ref} = reference value of normalized cone resistance, often taken at undrained conditions, $Q_{undrained}$ which normally occurs at maximum B_q. The value of normalized velocity when excess porewater pressures are half their maximum values is designated as a reference value, V_{50}. Finally, the exponent c is a fitting parameter.

Following a similar representation for Δu_2, a modified version of the algorithm for normalized porewater pressures given by DeJong et al. (2013) can be expressed by:

$$\frac{B_q}{B_{q-ref}} \approx 1 - \frac{1}{1 + (V/V_{50})^c} \qquad (52)$$

The fitting parameters for the centrifuge CPTs in kaolin shown as red dashed lines in Figures 31 and 32 are: $Q_{drained} = 7$; $Q_{ref} = Q_{undrained} = 3.2$, $V_{50} = 6$, c = 1, and $B_{q\text{-}ref} = 0.55$.

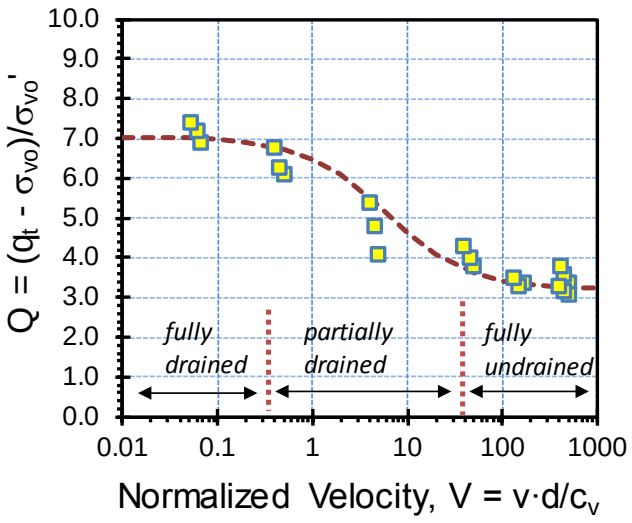

Figure 31. Centrifuge CPT cone resistance versus normalized velocity in kaolin (data from Schneider et al. 2007)

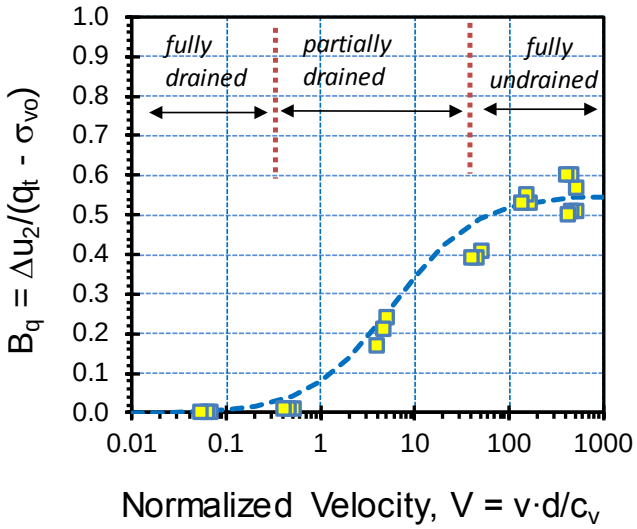

Figure 32. Centrifuge CPT porewater pressure response versus normalized velocity in kaolin (data from Schneider et al. 2007)

9.2 *Soil behavioral charts in Q-B_q space*

As noted earlier in Sections 2.1 and 2.2, results from piezocone tests can be plotted in Q-B_q space to ascertain soil behavioral type (SBT). As noted by Schneider (2009) and DeJong et al. (2013), these empirical charts are based on CPT data taken at the standard rate of 20 mm/s. Changes in CPT results due to rate effects will not be recognized by these SBT charts. Thus, the only valid points from the centrifuge tests for soil identification are the paired Q and B_q values from the undrained range, as shown in Figure 33. As the rate is decreased, the data appear to shift up and to the left into the silt mixture zone.

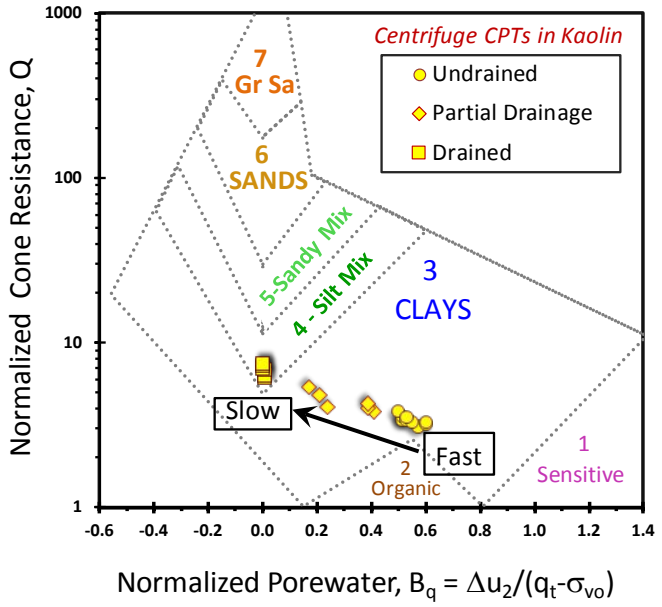

Figure 33. Centrifuge CPT data from twitch testing in kaolin plotted in SBT Q-B_q space.

9.3 *NTH solution presented in Q-B_q space*

For the case where c' = 0, the NTH solution is simply expressed in terms of normalized cone resistance and porewater pressure parameter. Thus, an alternate means of presenting the NTH solution of Figure 8 is in the format of the soil behavioral chart of Q versus B_q, as suggested by Ouyang et al. (2016) and illustrated in Figure 34.

The twitch test data from the CPT centrifuge experiments in kaolin are also shown and interestingly they more or less follow the same trends as the individual lines for specific ϕ' values. Since effective stress friction angle is a soil property, this should logically be expected with the same ϕ' realized in both the undrained and drained regions, as well as for intermediate partially drained cases.

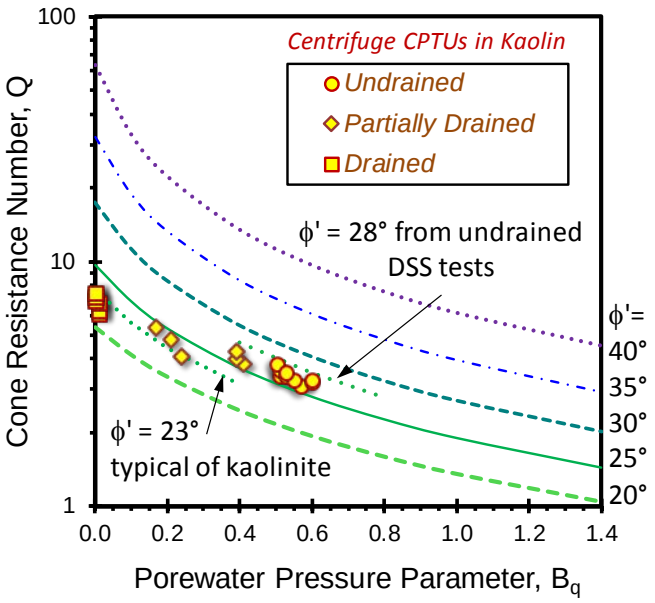

Figure 34. NTH solution for effective friction angle presented in Q-B_q space. Data from CPT twitch testing in centrifuge kaolin deposits also shown.

The specific kaolin used in the centrifuge CPTu twitch testing program has an apparent effective stress friction angle ϕ' = 28°, as determined from the τ-σ_v' plots from undrained simple shear tests reported by Schneider (2009). For the undrained Q and B_q values, this gives rather good agreement, as evident in Figure 34. Then, as the CPTu penetration rates are decreased, the resulting increase in Q and corresponding decrease in B_q show an apparent reduction in friction angle towards a value ϕ' = 23°. This value is more in line with the well-known values for kaolinite and mineral version of kaolin, as discussed by Rossato et al. (1992) and Section 8.2.

The reasons behind this trend are not clearly understood at this time, but perhaps relate to a change in the angle of plasticification (β) as the relative size of the failure region around the cone tip morphs from undrained to partially drained to drained conditions. Certainly additional research is needed to clarify this issue.

10 DISCUSSION

Several alternate theoretical solutions to represent cone penetration in clays have been documented (Konrad & Law 1987; Yu & Mitchell 1998; Low 2009). The choice of the Vesić (1977) cavity expansion solution was selected herein because a cone bearing factor $N_{kt} \approx 12 \pm 1$ associates with characteristic values of the porewater pressure parameter in soft clays: $B_q \approx 0.6 \pm 0.1$. Other solutions may prove more compatible in matching with available data in future studies (e.g., Lu et al. 2004; Low 2009;

Schneider et al. 2012). Certainly, more complex algorithms are necessary to represent the porewater pressure response of sensitive clays ($B_q > 0.8$) and overconsolidated clays ($B_q < 0.4$), as well as fissured fine-grained geomaterials ($B_q < 0$). For instance, one approach is a hybrid SCE-CSSM approach (Burns & Mayne 2002).

With regard to undrained effective stress penetration, the NTH solution appears to be a unique analytical approach for CPTu in clays for assessing ϕ'. An empirical approach has been proposed by Keaveny & Mitchell (1986), however received less attention.

Finally, it is perhaps necessary to utilize numerical finite element or finite difference schemes (e.g., Abu-Farsakh et al. 2003) in a means to advance CPTu interpretations forward in an effective stress framework in order to detail a universal approach for evaluating ϕ' in overconsolidated clays, as well as the full range of soil materials encountered in geotechnics. These numerical solutions should be well calibrated with extensive series of penetration tests at various rates and include dissipatory porewater pressure versus time measurements for a comprehensive set of data, e.g. CPTu and piezoball data reported by Mahmoodzadeh Randolph (2014).

11 CONCLUSIONS

Results from in-situ piezocone (CPTu) and flat dilatometer tests (DMT) in clays have traditionally been utilized for assessing total strength parameters, namely the undrained shear strength (s_u), often employed in limit equilibrium analyses and closed-form plasticity solutions for bearing capacity. Yet, modern geotechnical capabilities include finite element and finite difference modeling that require effective stress parameters (c' and ϕ'), thus giving the ability to predict field induced porewater pressure responses during construction.

As a consequence, it is of interest to review an existing NTH undrained effective stress limit plasticity solution for CPTu penetration in clays. This offers a means for evaluating ϕ' in soft clays (c' = 0), or alternatively a paired set of c' and ϕ' strength parameters. The NTH solution is extended to the DMT domain via links established from spherical cavity expansion (SCE) theory. Furthermore, interpretative procedures for clay stress history from CPTu readings can also be applied to DMT soundings. Laboratory and in-situ test results from the Bothkennar soft clay test site in the UK and data from other testing programs on clays are employed to illustrate the methodologies.

12 ACKNOWLEDGMENTS

The author appreciates the continued support of ConeTec Investigations of Richmond, BC and Design House Consultancy of New York, NY. Additional funding was provided by Fugro Engineers in Leidschendam, the US Dept. of Energy at Savannah River Site, and the Georgia Dept. of Transportation at Forest Park, Georgia USA.

13 REFERENCES

Abu-Farsakh, M., Tumay, M. & Voyiadjis, G. 2003. Numerical parametric study of piezocone penetration test in clays. *International J. of Geomechanics* Vol. 3 (2): 170-181.

Allman, M.A. & Atkinson, J.H. 1992. Mechanical properties of reconstituted Bothkennar soil. *Géotechnique* 42 (2): 289–301.

Baligh, M.M. 1986. Undrained deep penetration: pore pressures. *Geotechnique* 36 (4): 487-501.

Burns, S.E. & Mayne, P.W. 2002. Analytical cavity expansion-critical state model for piezocone dissipation in fine-grained soils. *Soils & Foundations* 42 (2): 131-137.

Chen, B.S.Y. and Mayne, P.W. 1993. Piezocone evaluation of undrained shear strength in clays. *Proc. 11th Southeast Asian Geotechnical Conference*, National Univ. of Singapore & Nanyang Technological Univ., Singapore: 91-98.

DeGroot, D.J., Lunne, T. & Tjelta, T.I. (2011). Recommended best practice for geotechnical site characterization of cohesive offshore sediments. Frontiers in Offshore Geotechnics II (Perth), Taylor & Francis, London: 33-57.

DeJong, J.D., Jaeger, R.A., Boulanger, R.W., Randolph, M.F. & Wahl, D.A.J. 2013. Variable penetration rate cone testing for characterization of intermediate soils. *Geotechnical & Geophysical Site Characterization 4*, Vol. 1 (Proc. ISC-4, Pernambuco), Taylor & Francis Group, London: 25-42.

Diaz-Rodriguez, J.A., Leroueil, S. & Aleman, J.D. 1992. Yielding of Mexico City clay and other natural clays. *J. Geotech. Engineering* 118 (7): 981-995.

Fellenius, B. H., & Eslami, A., 2000. Soil profile interpreted from CPTu data. *Proc. Geotechnical Engineering Conf.*, Asian Institute of Technology, Bangkok, Thailand, 18 p.

Finno, R.J. 1993. Analytical interpretation of dilatometer penetration in cohesive soils. *Geotechnique* 43(2): 241-254.

Ghalib, A., Hryciw, R., & Susila, E. 2000. Soil stratigraphy delineation by VisCPT. *Innovations & Applications in Geotechnical Site Characterization* (GSP No. 97), ASCE, Reston/VA: 65-79.

Hight, D.W., Böese, R., Butcher, A.P., Clayton, C.R.I. & Smith, P.R. 1992. Disturbance of the Bothkennar clay prior to laboratory testing. *Geotechnique* 42 (2): 199-217.

Hight, D.W., Paul, M.A., Barras, B.F., Nash, D.F.T., Smith, P.R., Jardine, R.J. & Edwards, D.H. 2003. The characterisation of the Bothkennar clay. Characterization & Engineering Properties of Natural Soils, Vol. 1, Swets & Zeitlinger, Lisse: 543-597.

Holtz, R.D., Kovacs, W.D. & Sheahan, T.C. 2011. *An Introduction to Geotechnical Engineering, 2nd Edition*, Pearson Educational, Upper Saddle River, NJ: 853 p,

Jamiolkowski, M., Ladd, C.C., Germaine, J.T. & Lancellotta, R. 1985. New developments in field and lab testing of soils. *Proc. 11th ICSMFE*, San Francisco: 57-153.

Keaveny, J.M. & Mitchell, J.K. 1986. Strength of fine-grained soils using the piezocone. *Use of In-Situ Tests in Geot. Engrg*, GSP 6, ASCE, Reston, Virginia: 668-685.

Konrad, J-M. & Law, K.T. 1987. Undrained shear strength from piezocone tests. *Canadian Geot. J.* 24 (3): 392-405.

Larsson, R. & Åhnberg, H. 2005. On the evaluation of undrained shear strength and preconsolidation pressure from common field tests in clay. *Canadian Geotechnical J.* 42 (4): 1221-1231.

Locat, J., Tanaka, H., Tan, T.S., Dasari, G.R. and Lee, H. 2003. Natural soils: geotechnical behavior and geological knowledge. *Characterization & Engrg. Properties of Natural Soils*, Vol. 1, Swets & Zeitlinger, Lisse: 3-28.

Low, H.E. 2009. Performance of penetrometers in deepwater soft soil characterisation. *PhD Thesis*. Centre for Offshore Foundation Systems, School of Civil & Resource Engrg., Univ. Western Australia: 300 p.

Low, H.E., Lunne, T., Andersen, K.H., Sjursen, M.A., Li, X. and Randolph, M.F. 2010. Estimation of intact and remoulded undrained shear strengths from penetration tests in soft clays. *Geotechnique* 60 (11): 843-859.

Lu, Q., Randolph, M.F., Hu, Y. & Bugarski, I.C. 2004. A numerical study of cone penetration in clay. *Geotechnique* 54 (4): 257-267.

Lunne, T., Robertson, P.K., and Powell, J.J.M. 1997. *The Cone Penetration Test in Geotechnical Practice*, EF Spon/Blackie Academic, Routledge Publishing, New York: 312 p.

Lunne, T., Randolph, M.F., Chung, S.F., Andersen, K.H. and Sjursen, M. 2005. Comparison of cone and t-bar factors in two onshore and one offshore clay sediments. *Frontiers in Offshore Geotechnics* (Proc. ISFOG-1, Perth), Taylor & Francis Group, London: 981-989.

Lunne, T. (2010). The CPT in offshore soil investigations - a historic perspective. *Proc. 2nd Intl. Symp. on Cone Penetration Testing*, Vol. 1, Huntington Beach, CA; Omnipress: 71-113. www.cpt10.com

Marchetti, S. 1980. In-situ tests by flat dilatometer. *Journal of Geotechnical Engrg.* 106 (GT3): 299–321.

Marchetti, S., Monaco, P., Totani, G. & Calabrese, M. 2001. The flat dilatometer test (DMT) in soil investigations. A report by the ISSMGE Committee TC16. Reprinted in *Proc. 3rd Intl. Conf. on the Flat Dilatometer*, Rome: 523-565.

Marchetti, D., Marchetti, S., Monaco, P. & Totani, G. 2008. Experience with seismic dilatometer in various soil types. *Geotechnical & Geophysical Site Characterization*, Vol. 2 (ISC-3, Taiwan), Taylor & Francis, London: 1339-1345.

Marchetti, S. 2015. Update. *Proceedings 3rd Intl. Conf. on Flat Dilatometer*. Rome: 299–321. www.dmt15.com

Mayne, P.W. & Stewart, H.E. 1988. Pore pressure response of K_0-consolidated clays. *Journal of Geotechnical Engineering*, Vol. 114 (11): 1340-1346.

Mayne, P.W. & Bachus, R.C. 1989. Penetration porewater pressures in clay by CPTU, DMT, and SBP. *Proc., 12th Intl. Conf. on Soil Mech. & Foundation Engineering*, Vol. 1, Rio de Janeiro: 291-294.

Mayne, P.W. 1991. Determination of OCR in clays by piezocone tests using cavity expansion and critical state concepts. *Soils and Foundations*, Vol. 31 (2), June: 65-76.

Mayne, P.W. 2001. Stress-strain-strength-flow parameters from enhanced in-situ tests. *Proc. International Conf. on In-Situ Measurement of Soil Properties & Case Histories* (In-Situ 2001), Bali, Indonesia: 27-47.

Mayne, P.W., Christopher, B., Berg, R., and DeJong, J. 2002. *Subsurface Investigations - Geot. Site Characterization*. Publication No. FHWA-NHI-01-031, National Highway Institute, Federal Highway Admin., Washington, D.C., 301 p

Mayne, P.W. 2006. Interrelationships of DMT and CPTU readings in soft clays, *Flat Dilatometer Testing* (Proc. 2nd Intl. Conf. DMT), Washington, DC: 231-236.

Mayne, P.W. 2007. In-situ test calibrations for evaluating soil parameters, *Characterization & Engineering Properties of Natural Soils*, Vol. 3 (Proc. Singapore 2006), Taylor & Francis Group, London: 1602-1652.

Mayne, P.W. 2007. *Synthesis 368 on Cone Penetration Test*. (NCHRP), Transportation Research Board, National Academy Press, Washington DC: 120 p. www.trb.org

Mayne, P.W., Coop, M.R., Springman, S., Huang, A-B., & Zornberg, J. 2009. SOA-1: Geomaterial behavior and testing. Proc. *17th Intl. Conf. Soil Mechanics & Geot. Engrg*., Vol. 4 (ICSMGE, Alexandria), Millpress/IOS Press, Rotterdam: 2777-2872.

Mayne, P.W. 2012. Invited keynote: Quandary in geomaterial characterization: new vs. old. *Shaking the Foundations of GeoEngineering Education* (Proc. Univ. Ireland, Galway), Taylor & Francis Group, London: 15-26.

Mayne, P.W. 2013. Updating our geotechnical curricula via a balanced approach of in-situ, laboratory, and geophysical testing of soil. *Proc. 61st Annual Geotechnical Conference*, Minnesota Geot. Society, Univ. Minnesota, St. Paul: 65-86.

Mayne, P.W. 2014. Keynote: Interpretation of geotechnical parameters from seismic piezocone tests. *Proceedings, 3rd Intl. Symposium on Cone Penetration Testing*, (CPT'14, Las Vegas): 47-73. www.cpt14.com

Mayne, P.W. and Peuchen, J. 2012. Unit weight trends with cone resistance in soft to firm clays. *Geotechnical and Geophysical Site Characterization 4*, Vol. 1 (Proc. ISC-4, Pernambuco), CRC Press, London: 903-910.

Mayne, P.W., Peuchen, J. & Baltoukas, D. 2015. Piezocone evaluation of undrained strength in soft to firm offshore clays. *Frontiers in Offshore Geotechnnics III*, Vol. 2 (Proc. ISFOG-3, Oslo), Taylor & Francis, London: 1091-1096.

Mayne, P.W. 2015. Keynote lecture: In-situ geocharacterization of soils in the year 2016 and beyond. *Advances in Soil Mechanics, Vol. 5: Geotechnical Synergy* (Proc. PCSMGE, Buenos Aires), IOS Press, Amsterdam: 139-161.

Mesri, G. & Abdel-Ghaffar, M.E.M. 1993. Cohesion intercept in effective stress-stability analysis. *J. Geotechnical Engineering* 119 (8): 1229-1249.

Mahmoodzadeh, H. & Randolph, M.F. 2014. Penetrometer testing: effect of partial consolidation on subsequent dissipation response. *J. Geotechnical & Geoenviron. Engrg*. Vol. 140 (6), 04014022.

Nash, D.F.T., Powell, J.J.M. & Lloyd, I.M. 1992a. Initial investigations of the soft clay testbed site at Bothkennar clay site. *Géotechnique* 42(2): 163–181.

Nash, D.F.T., Sills, G.C. & Davison, L.R. 1992b. One-dimensional consolidation testing of soft clay from Bothkennar. *Geotechnique* 42 (2): 241-256.

Ouyang, Z., Mayne, P.W. & Sharp,.J. 2016. Review of clay chamber tests using miniature cone and piezocone penetrometers, *Proc. GeoVancouver 2016*, (69th Canadian Geotechnical Conference): www.cgs.ca

Powell, J.J.M. & Lunne, T. 2005. A comparison of different sized piezocones in UK clays. *Proc. ICSMGE*, Vol. 1 (Osaka), Millpress/IOS, Rotterdam: 729-734.

Randolph, M.F. 2004. Characterization of soft sediments for offshore applications. *Geotechnical & Geophysical Site Characterization*, Vol. 1 (Proc. ISC-2, Porto), Millpress, Rotterdam: 209-232.

Robertson, P.K. 2009. Cone penetration testing: a unified approach. *Canadian Geotechnical J.* 46 (11): 1337-1355.

Rossato, G., Ninis, N., and Jardine, R.1992. Properties of some kaolin-based model clay soils. *Geotechnical Testing Journal*, Vol. 15, No. 2, ASTM: 166-179.

Sandven, R. 1990. Strength and deformation properties of fine grained soils obtained from piezocone tests. *PhD Dissertation*, Institutt for Geoteknikk, Norwegian Inst. of Technology (NTH), Trondheim: 600 p.

Sandven, R. & Watn, A. 1995. Soil classification and parameter evaluation from piezocone tests. Proc. 2nd Intl. Symp. on Cone Penetration Testing (CPT'95, Linköping), Vol. 3, Swedish Geotechnical Society: 35-55.

Schneider, J.A. 2009. Separating influences of yield stress ratio and partial drainage on piezocone response. *Australia Geomechanics Journal* 44 (3): 1-18.

Schneider, J.A., Lehane, B.M. & Schnaid, F. 2007. Velocity effects on piezocone measurements in normally and overconsolidated clays. *Intl. J. of Physical Modelling in Geotechnics*, Vol. 7, Issue 2: 23-34.

Schneider, J.A., Randolph, M.F., Mayne, P.W., & Ramsey, N.R. 2008. Analysis of factors influencing soil classification using normalized piezocone tip resistance and pore pressure parameters. *Journal of Geotechnical & Geoenvironmental Engrg*. 134 (11): 1569-1586.

Schneider, J.A., Hotstream, J.N., Mayne, P.W. & Randolph, M.F. 2012. Comparing CPTu Q-F and Q-$\Delta u_2/\sigma_{vo}'$ soil classification charts. *Geotechnique Letters*, Vol. 2 (4): 209-215.

Schofield, A.N. & Wroth, C.P. 1968. *Critical State Soil Mechanics*, McGraw-Hill, London: 310 p. Download PDF version from: www.geotechnique.info

Senneset, K. & Janbu, N. 1985. Shear strength parameters obtained from static cone penetration tests. *Strength Testing of Marine Sediments*. Special Tech Publ. 883, ASTM, West Conshohocken, PA: 41-54.

Senneset, K., Sandven, R. & Janbu, N. 1989. Evaluation of soil parameters from piezocone tests. *In-Situ Testing of Soil Properties for Transportation, Transportation Res. Record 1235*. National Research Council, Washington DC: 24-37.

Sorensen, K.K. & Okkels, N. 2013. Correlation between drained shear strength and plasticity index of undisturbed overconsolidated clays. *Proc. 18th Intl. Conf. Soil Mech. & Geot. Engrg.*, Paris: 423-428.

Torrez-Cruz, L.A. 2015. CPT-based soil type classification in a platinum tailings storage facility. *From Fundamentals to Applications in Geotechnics*, Part 1 (Proc. 15th PCSMGE, Buenos Aires), IOS Press, Rotterdam: 406-413.

Tümay, M.T., HatipKarasulu, Y., Młynarek, Z., & Wierzbicki, J. 2011. Effectiveness of CPT-based classification methods for identification of subsoil stratigraphy. *Proc. 15th European Conf. on Soil Mechanics & Geot. Engineering*, Athens, Greece, Vol. 1, IOS/Millpress, Rotterdam: 91-98.

Vesić, A.S. 1972. Expansion of cavities in infinite soil mass. *Journal of the Soil Mechanics & Foundations Division* (ASCE), Vol. 98 (SM3): 265-290.

Vesić, A.S. 1977. *Design of Pile Foundations, NCHRP Synthesis No. 42*, Transportation Research Board, National Academy Press, Washington, DC: 68 pages.

Wood, D.M. 1990. *Soil Behaviour and Critical State Soil Mechanics*. Cambridge Univ. Press, UK: 462 p.

Yu, H.S. & Mitchell, J.K. 1998. Analysis of cone resistance: review of methods. *J. Geotechnical & Geoenvironmental Engineering* 124 (2): 140-149.